International Journal of Electronics, Mechanical and Mechatronics Engineering (IJEMME) is peer-reviewed journal which provides a platform for publication of original scientific research and applied practice studies. Positioned as a vehicle for academics and practitioners to share field research, the journal aims to appeal to both researchers and academicians.
Internationally indexed by EBSCO and DOAJ

CONTENTS

From Editor

Engineering Faculty of Istanbul Aydın University has started to publish an international journal on Electronics, Mechanical and Mechatronics Engineering, denoted as "International Journal of Electronics, Mechanical and Mechatronics Engineering (IJEMME)". We have especially selected the scientific areas which will cover future prospective engineering titles such as Robotics, Mechanics, Electronics, Telecommunications, Control Systems, System Engineering, Biomedical, and Renewable Energy Sources.

We have selected only a few of the manuscripts to be published after a peer review process of many submitted studies. Editorial members aim to establish an international journal IJEMME, which will be welcomed by Engineering Index (EI) and Science Citation Index (SCI) in short period of time.

Prof. Dr. Zafer UTLU
Editor

Comparison of Sinusoidal and Space Vector PWM Control Techniques for Three-Level Inverter Drives

Ayse KOCALMIS BILHAN[1]
Sedat SUNTER[2]

Abstract

In recent years, inverters have been the most popular part of electrical drivers in variable voltage and frequency applications. Also multilevel inverters have gained interest in high power applications because of their advantages in high voltage and high power levels with low harmonic content. In this paper, basic structure of three-level inverter is introduced and its two modulation strategies are compared. One of the modulation algorithms is SPWM (Sinusoidal Pulse Width Modulation) technique where a sinusoidal modulation signal is compared with two triangle signals to obtain the three-level at the output phase voltage of the inverter. A simple SVPWM (Space Vector Pulse Width Modulation) algorithm is also realized. In this technique, three nearest vectors can be selected easily and switching sequence and switching times are calculated by using the vector position. Both techniques are simulated by using MATLAB/Simulink package program and applied to the RL and motor loads. Comparative results are given.

Keywords: Inverters, pulse width modulation inverters, space vector pulse width modulation

1. Introduction

In industries, where variable speed drives are required, induction motor drives are important. There are vairous strategies for control such as scalar control, vector control or field oriented control. In the literature, the inverters with having three levels or more than three levels on their output phase voltages have been named as multilevel inverters [1-3]. Multilevel inverters (MLs) have been usually applied to high power medium voltage applications due to their low switching frequency and less total harmonic distortion (THD) [1, 4]. Voltage stress of the each switching device is reduced because of the voltage share on the circuit. Besides, their harmonic content is reduced in higher levels. For example, three-level structure has less harmonic content than that of two-level structure at the same switching frequency [4, 5]. A schematic diagram of an H-Bridge multilevel inverter is shown in Fig.1. Three-phase output voltage waveforms are generated by various switching combination of the switches in the H-bridge inverter. As a result, three-level at the output phase voltage waveforms is obtained as +E/2 V, 0 V, -E/2 V. Number of H-bridges of each phase can be increased for getting higher levels. Number of H-bridges for each phase can be calculated using Eq. (1). (where; m is number of the output voltage level).
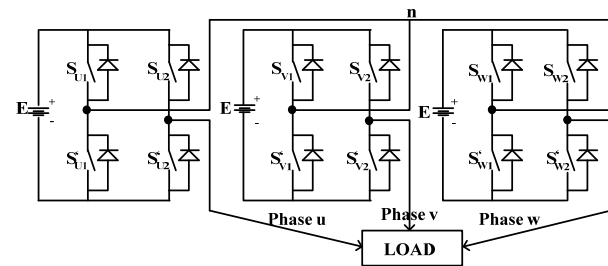
Figure 1. Three-phase three-level H-bridge inverter circuit

m is always an odd number in H-bridge multilevel inverter structure. The numbers of H-bridge are determined by considering the desired output voltage and harmonic contents [1, 6, 7].

$$H_{Bridge} = \frac{(m-1)}{2} \qquad (1)$$

In this paper, modeling and simulation of an H-bridge three-level inverter have been performed applying Sinusoidal Pulse Width Modulation (SPWM) and Space Vector Pulse Width Modulation (SVPWM) techniques with R-L and motor loads using Simulink/

[1] Nevsehir H.B.V. University, Nevsehir, Turkey, akbilhan@nevsehir.edu.tr

[2] Firat University, Elazig, Turkey

MATLAB package program. Comparison results of two methods are given respectively.

2. Analysis of SPWM Technique For Three-Level Inverter

In SPWM technique, Pulse Width Modulation (PWM) signals are generated by comparing a sinusoidal signal (reference signal magnitude is V_{Ref} and frequency f_{Ref}) with a triangle signal (carrier signal magnitude is $V_{carrier}$ and frequency f_C) [8]. To increase the number of output levels, number of carrier signal is increased keeping the reference signal. Number of carrier signal ($N_{carrier}$) and modulation index (M_i) are given in Eq. (2) and (3), respectively.

$$N_{carrier} = m-1 \qquad (2)$$

$$M_i = \frac{\hat{V}_{Ref.}}{(a-1)\hat{V}_{Car.}} \qquad (3)$$

The carrier signals and reference signals are compared as shown in Fig.2 in three-level SPWM.
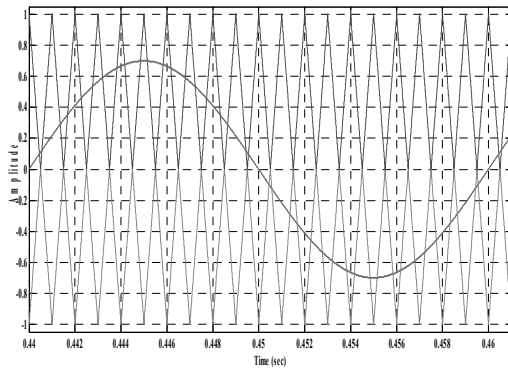
Figure 2. Three-Level SPWM

Analog implementation of this technique is hardly used now. Because, pulse widths are solutions to transcendental equations so that it is not suitable for microprocessor applications. Instead regular sampling is used where the reference signal is sampled and held at a frequency of fc or 2 fc. The sampled signal is then compared with the carrier signal. Interest in other PWM techniques has been also increased. Selective Harmonic Elimination PWM (SHEPWM) [9], minimum current ripple PWM, third harmonic injection PWM (THIPWM) [10] are some alternatives of the PWM techniques. However, space vector PWM (SVPWM) technique is recently showing popularity for inverter applications [1, 11-14].

3. Analysis of SVPWM Technique for Three-Level Inverter

Main aim of modulation techniques is to get less harmonic distortion, less switching losses and large modulation ratio. For this reason, many modulation techniques have been improved. Recently, SVPWM technique has become more popular because of achieving the goals mentioned above. Besides these advantages of SVPWM, it has some disadvantages such as complex calculation procedures [15, 16]. Switching states and active voltage levels can be calculated by using Eq. (4) and (5).

$$A = m^3 \qquad (4)$$

$$A_{Active} = 1 + 6\sum_{i=1}^{m-1} i \qquad (5)$$

In each phase, there are four switching devices each having anti parallel diodes as shown in Fig.1. There are $3^3 = 27$ switching states for three-level H-bridge SVPWM. Every switching states can be represented as a voltage level by using Eq. (3). Three of them (111, 000, -1-1-1) are zero voltage vectors and they are centered in the middle of the space vector hexagon. Other switching states are active voltage vectors and they are located in the different part of hexagon. Possibilities for all switching states are given in Fig.3. Also switching states of the three-level inverter is listed in Table1. x represents u, w and z phases, respectively [15-17].

Table 1. Switching States of Three-Level Inverters (x=u, w, z phases)

S_{X0}	S_{X1}	S_{X2}	S'_{X1}	S'_{X2}
+E/2V	on	off	off	on
0V	on	on	off	off
0V	off	off	on	on
-E/2V	off	on	on	off

Fig.3 shows space vector diagram of the three-level inverter. As can be seen, the hexagon is divided into six portions and every portion is divided into four different parts. The portions are named as Sectors (Sector A, Sector B,…, Sector F) and four parts are named as region (Region 1,…, Region 4) [14, 18, 19].

Output voltage is produced by using three adjacent vectors. Eq. (8) shows how to calculate the output voltage, V*.

$$T_U V_U + T_V V_V + T_W V_W = T_S V^*$$
$$T_U + T_V + T_W = T_S \qquad (6)$$

where; T_S is the sampling time, V_U, V_V, and V_W are three adjacent vectors and T_U, T_V and T_W are vector duration times. Vector, V^* falls into one of the six sectors depending on the vector angle, θ and it is calculated by using Eq. (7) and (8). V_α and V_β are used to determine the reference vector. The three-phase variables transforms to equivalent two-phase variables. Table 2 defines the sectors and their regions. [20-22].

$$V^* = V_\alpha + jV_\beta = \frac{2}{3}(V_U e^{j0} + V_V e^{\frac{j2\pi}{3}} + V_W e^{\frac{j4\pi}{3}}) \qquad (7)$$

$$\theta = \arctan^{-1}(\frac{V_\beta}{V_\alpha}) \qquad (8)$$

The other important issue is to estimate position of the voltage vector (V^*) correctly. To achieve this, some geometrical equations illustrated in Fig.4 and given with Eq. (9-10) are used.
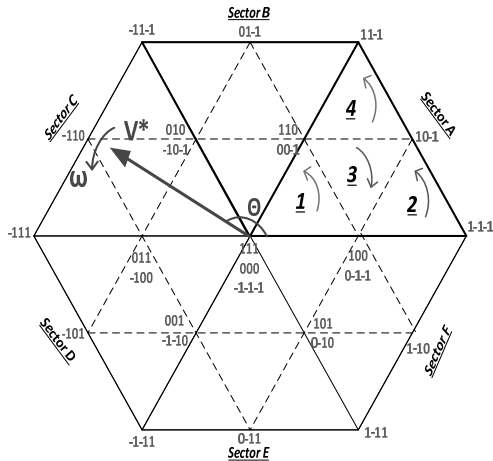
Figure 3. Space Vector Diagram of Three-Level Inverter

Table 2. V^* Position in Three-Level SVPWM Diagram

Angle(Θ)	Sector
$0° \leq \Theta < 60°$	Sector A
$60° \leq \Theta < 120°$	Sector B
$120° \leq \Theta < 180°$	Sector C
$180° \leq \Theta < 240°$	Sector D
$240° \leq \Theta < 300°$	Sector E
$300° \leq \Theta < 360°$	Sector F
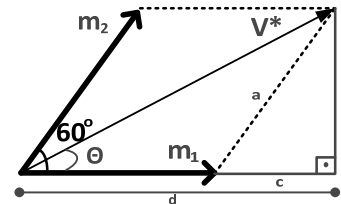
Figure 4. Estimating position of V^*

$b = m_n \sin\theta$ and $b = a\sin\theta$

$$a = m_2 = \frac{b}{\sin 60} = \frac{2}{\sqrt{3}} b = \frac{2}{\sqrt{3}} V^* \sin\theta \qquad (9)$$

$m_1 = d - c$

$$m_1 = V^* (\cos\theta - \frac{\sin\theta}{\sqrt{3}}) \qquad (10)$$

It is important to notice that only one switching device is at any time. The switching sequences for each region located in Sector A are given below using all switching states. "1" represents $+E/2$ V, "0" represents 0 V, and "-1" represents $-E/2$ V output voltage levels. Therefore, switching signals for Sector A are [14, 23, 24];

Region 1:-1-1-1, 0-1-1, 00-1, 000, 100, 110, 111, Region 2:0-1-1, 1-1-1, 10-1, 100, Region 3: 0-1-1, 00-1, 10-1, 100, 110, Region 4:00-1, 10-1, 11-1, 110,

Fig.5 shows switching states and times for Sector A [1, 14, 25].
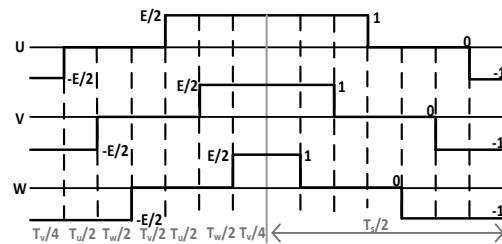
(a) Region 1
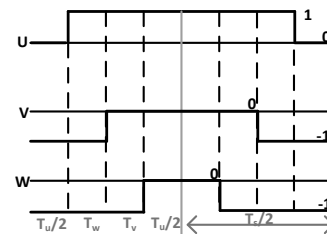
(b) Region 2
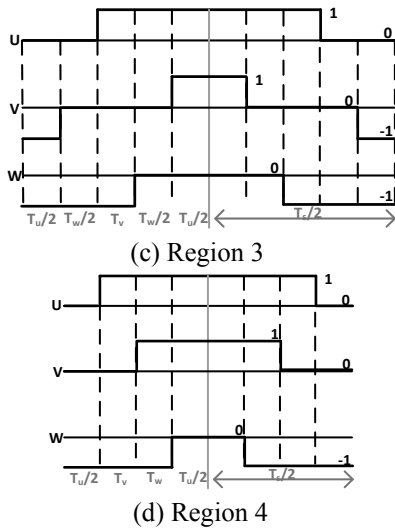
(c) Region 3

(d) Region 4

Figure 5. Switching signals of Sector A for all regions

For three-level SVPWM, space vector diagram and equations for switching times in Sector A is given in Fig.6 and Table 3, respectively.
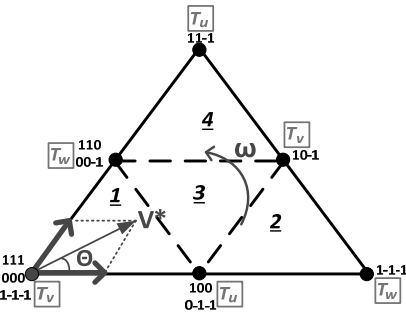
Figure 6. Space vector diagram of Sector A

Table 3. Switching Times and Equations of Sector A For Three-Level SVPWM

Switching Times	Region 1
T_u	$n*T_s*\sin((\pi/3)-\Theta)$
T_v	$T_s/2(1-(2*n*\sin(\Theta+\pi/3))$
T_w	$n*T_s*\sin\Theta$
	Region 2
T_u	$T_s(1-n*\sin(\Theta+\pi/3))$
T_v	$T_s*n*\sin\Theta$
T_w	$T_s/2((2*n*\sin(\pi/3-\Theta))-1)$
	Region 3
T_u	$T_s/2(1-2*n*\sin\Theta)$
T_v	$T_s/2(2*n*\sin(\pi/3+\Theta)-1)$
T_w	$T_s/2(1+2*n*\sin(\Theta-\pi/3))$
	Region 4

T_u	$T_s/2(2*n*\sin(\Theta)-1)$
T_v	$n*T_s*\sin((\pi/3)-\Theta)$
T_w	$T_s(1-(n*\sin(\Theta+\pi/3))$

where n is constant. m_{SVPWM} is a modulation index of SVPWM and it is defined as;

$$m_{SVPWM}=\frac{\sqrt{3}}{2}\frac{V^*}{V_E} \tag{11}$$

4. Modelling and Simulation

Fig.7 shows MATLAB/Simulink model of the whole system for both SPWM and SVPWM techniques. "A Phase", "B Phase" and "C Phase" blocks in Fig.7 contain H-bridge inverter structures. In these blocks, output voltages are synthesized. "E Source", "E Source1" and "E Source2" blocks are independent DC voltage source blocks. They are input to each H-bridge inverters and they are all isolated from each other. "Switching Signals of Phase A", "Switching Signals of Phase B" and "Switching Signals of Phase C" blocks produce switching signals using SPWM and SVPWM techniques as explained in the previous sections.
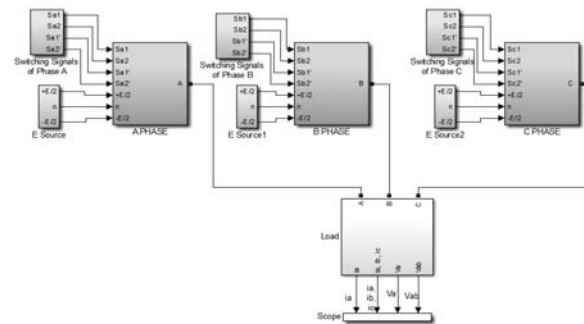
Figure 7. Simulation model of the whole system

In Fig.8 (a) and (b), basic structure of "Switching Signals of Phase" blocks applying SPWM and SVPWM techniques has been shown, respectively.

(a)

(b)
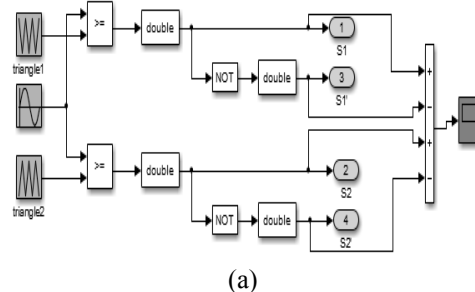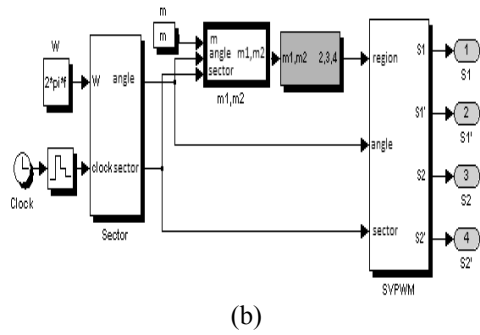
Figure 8. Producing Switching Signals (a) SPWM (b) SVPWM

Simulation results for both SPWM and SVPWM methods have been taken for various operating conditions. A passive load of R=100 Ω and L=0.1 H and motor load are used to demonstrate the performance of the inverter controlled by SPWM and SVPWM algorithms. The motor parameters are given in Appendix. Switching frequency of 1 kHz is used in the model. DC link voltage of the cascade inverters is taken as 500 V.

Simulation results shown in Fig.9 through Fig.11 have been obtained for modulation index of 0.2 and 0.8 and output frequency of 10 Hz, 30 Hz and 70 Hz for SPWM and SVPWM with passive load.

(c)

(d)
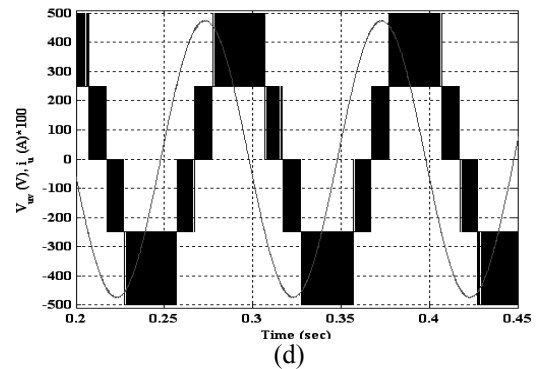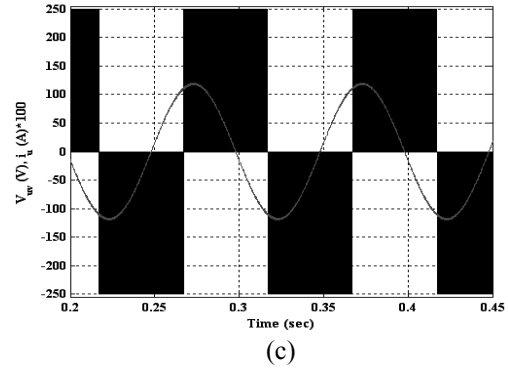
Figure 9. Simulation results of V_{ab} output line voltage and i_b phase current (x100) a) f=10 Hz and m=0.2 using SPWM,b) f=10 Hz and m=0.8 using SPWM, c) f=10 Hz and m=0.2 using SVPWM, d) f=10 Hz and m=0.8 using SVPWM for R=100 Ω, L=0.1 H passive load.

(a)

(a)

(b)

(b)

(a)

(c)

(b)

(d)

(c)
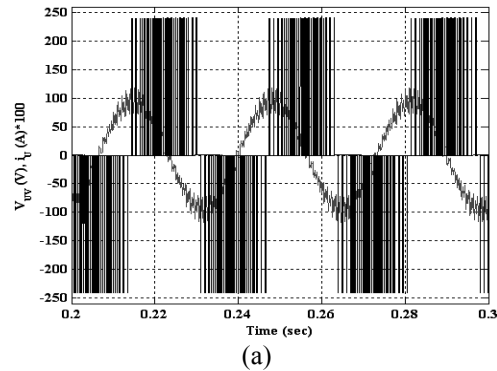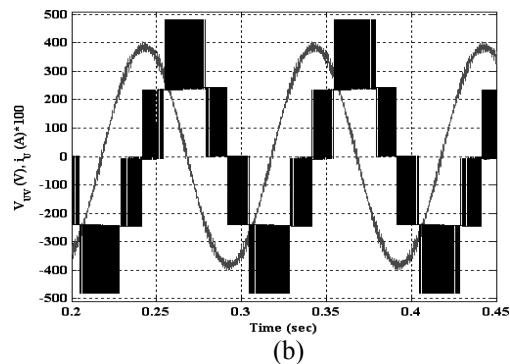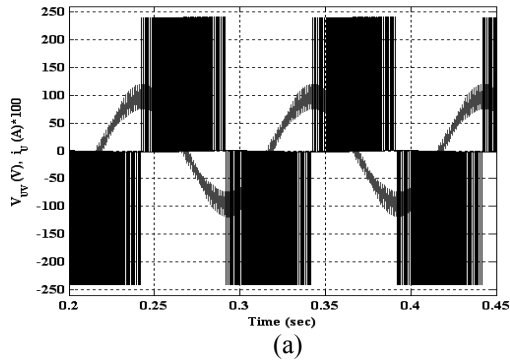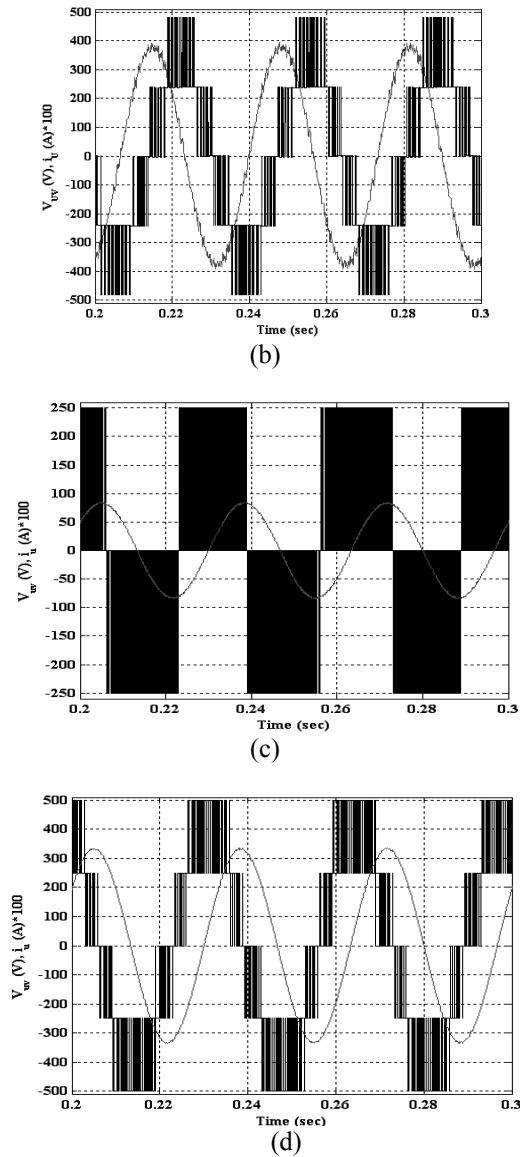
Figure 10. Simulation results of V_{ab} output line voltage and i_b phase current (x100) a) f=30 Hz and m=0.2 using SPWM,b) f=30 Hz and m=0.8 using SPWM, c) f=30 Hz and m=0.2 using SVPWM, d) f=30 Hz and m=0.8 using SVPWM for R=100 Ω, L=0.1 H passive load.

(d)
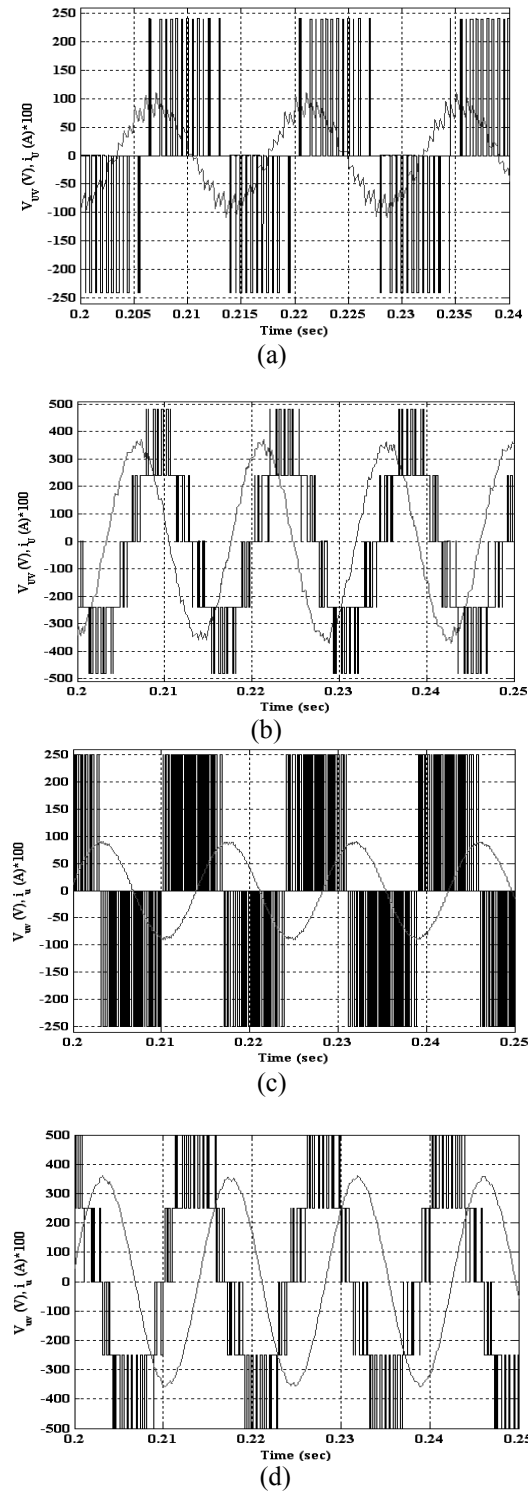
Figure 11. Simulation results of V_{ab} output line voltage and i_b phase current (x100) a) f=70 Hz and m=0.2 using SPWM, b) f=70 Hz and m=0.8 using SPWM, c) f=70 Hz and m=0.2 using SVPWM, d) f=70

Hz and m=0.8 using SVPWM for R=100 Ω, L=0.1 H passive load.

As can be seen from the results that the output voltage wave forms have three-level in lower modulation index of 0.2 and five-level in higher modulation index of 0.8.
As can be easily noticed that current waveforms with SVPWM have better sinusoidal shape for all conditions comparing to the current waveforms with SPWM. It can be also observed that operating range of SVPWM is higher than that of SPWM. As a result, SPWM uses bigger modulation index to get same output voltage as SVPWM. This is given in Eq.(12) as;

$$m_{SPWM} = \frac{4}{3} m_{SVPWM} \qquad (12)$$

In Fig.12 and Fig.13, simulation of SVPWM has been repeated for an induction motor load. The results have been taken at no-load conditions. Fig.12 shows motor phase current of phase-u fed by the three-level SVPWM inverter at 10 Hz output frequency. Modulation index (m_{SVPWM}) is taken as 0.2 to provide constant v/f operation in steady-state.

(a)

(b)
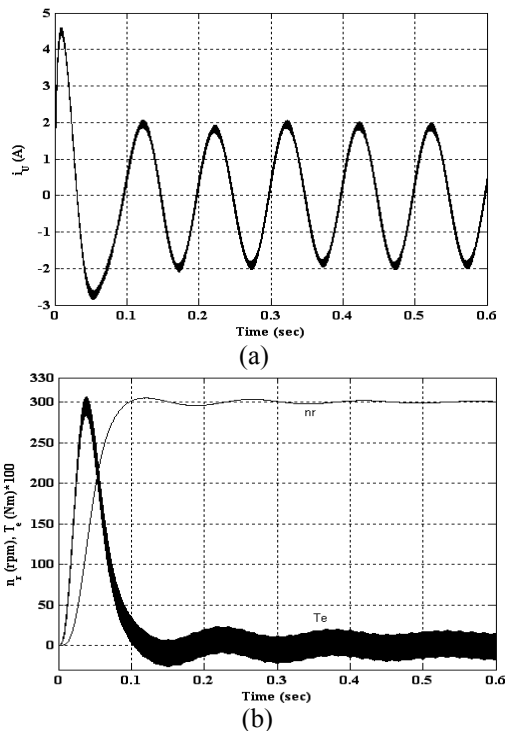
Figure 12. (a) Motor current waveform for phase-u, (b) Motor speed and electromagnetic torque for m=0.2 and f=10 Hz using SVPWM technique.

Fig.13 illustrates phase motor current and motor speed and torque waveforms for an output frequency of 70 Hz.

(a)

(b)
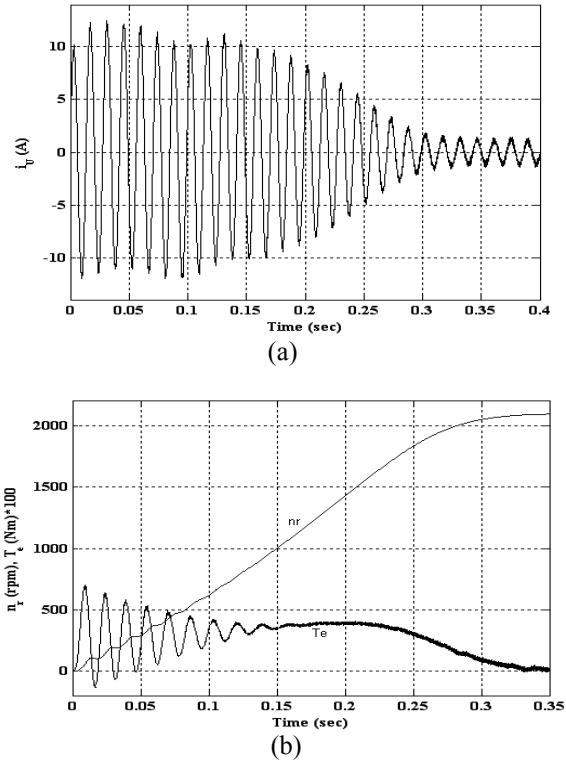
Figure 13. (a) Motor current waveform for phase-u, (b) Motor speed and electromagnetic torque for m=0.8 and f=70 Hz using SVPWM technique.

5. Conclusions
The space vector PWM method (SVPWM) and the sinusoidal PWM method (SPWM) for three level inverter using H-bridge topology have been modelled and simulated. Simulation results have been taken for R-L passive load and motor load for both methods. A proposed method (SVPWM) has shown better performance than classical conventional method (SPWM). From the results it is clear that, SVPWM gave less current ripple, THD than the SPWM modulation scheme. The proposed algorithm can be easily applied to multilevel inverters. It is more difficult to realize both digital and analog applications of SPWM method to multilevel inverters comparing to the SVPWM method. The proposed control algorithm given for the three-level inverter can be easily applied to multilevel inverters. It has been shown that high quality waveforms at the output of multilevel inverters can be reached by using proposed method.

Appendix

Ratings of the three-phase, 4-pole, 380 V, 50 Hz squirrel cage induction motor are:

Frequency range: 0-70 Hz, Stator resistance (Rs): 7 Ω, Rotor resistance (Rr): 6 Ω, Stator leakage inductance (Lσs): 0.52 mH, Rotor leakage inductance (Lσr): 0.52 mH, Magnetizing inductance (Lm): 0.5 mH, Rotor inertia (J): 0.0085 kgm^2, PN: 1.1 kW, TN: 7.62 Nm.

REFERENCES

[1] B.K., Bose, "Modern power electronics", 1983.

[2] J., Rodriguez, J.-S., Lai, F.Z., Peng, "Multilevel inverters: A survey of topologies, controls and applications", IEEE Trans. on Industrial Electronics, Vol. 49, No. 4, pp. 1631-1639, Aug. 2002.

[3] M., Manjrekar, G., Venkataramanan, "Advanced topologies and modulation strategies for multilevel inverters", Power Electronics Specialists Conference, Vol. 2, pp. 1013-1018, 23-27 June 1996.

[4] P.M., Bhagwat, V.R., Stefanovic, "Generalized structure of a multilevel inverter", IEEE Trans. on I.A., Vol. IA-19, n.6, pp. 1057-1069, 1983.

[5] N., Mohan, T.M., Undeland, W.P., Robbins, "Power electronics: converters, applications, and design", John Wiley & Sons, Inc., 1989.

[6] A.K., Gupta, A.M., Khambadkone, "A space vector pwm scheme for multilevel inverters based on two-level space vector pwm", IEEE Trans. on Industrial Electronics, Vol. 53, No. 5, Oct. 2006.

[7] G., Guo, W., You, "Quality analysis of svpwm inverter output voltage", IEEE International Conference on Computer Science and Software Engineering, pp. 126-129, 2008.

[8] C.S.Sharma, T., Nagwani, "Simulation and Analysis of PWM Inverter Fed Induction Motor Drive", Int. J. of Science, Engineering and Technology Research, Vol. 2, No. 2, pp. 359-366, 2013.

[9] B.P., McGrath, D.G., Holmes, "A comparison of multicarrier pwm strategies for cascaded and neutral point clamped multilevel inverters" IEEE Power Electronics Specialists Conference, Vol. 2, pp.674 – 679, 18-23 June 2000.

[10] W., Subsingha, "A Comparative Study of Sinusoidal PWM and Third Harmonic Injected PWM Reference Signal on Five Level Diode Clamp Inverter", Energy Procedia, Vol. 89, pp. 137-148, 2016.

[11] M.S.A., Dahidah, G., Konstantinou, V.G. Agelidis, "A Review of Multilevel Selective Harmonic Elimination PWM: Formulations, Solving Algorithms, Implementation and Applications", IEEE Trans. on Power Electronics, Vol. 30, No. 8, pp. 4091-4106, 2015.

[12] C., Zang, Z., Pei, J., He, T., Guo, J., Zhu, W., Sun, "Research on the application of CPS-SPWM technology in cascaded multilevel inverter", International Conference Electrical Machines and Systems, ICEMS, pp. 1-4, 2009.

[13] J., Pradeep, R., Devanathan, "Comparative analysis and simulation of pwm and svpwm inverter fed permanent magnet synchronous motor", International Conference on Emerging Trends in Electrical Engineering and Energy Management (ICETEEEM), pp. 299-305, 2012.

[14] A., Kocalmis, S., Sunter, "Simulation of a space vector pwm controller for a three-level voltage-fed inverter motor drive", IECON 2006-32nd Annual Conference on IEEE Industrial Electronics, pp. 1915–1920, 6-10 Nov. 2006.

[15] R., Rabinovici, D., Baimel, J., Tomasik, A., Zuckerberger, "Series space vector modulation for multi-level cascaded H-bridge inverters", Power Electronics, IET., pp. 843–857, 2010.

[16] J.H., Seo, C.H., Choi, D.S., Hyun, "A new simplified space–vector pwm method for three-level inverters", IEEE Trans. on Power Electronics, Vol. 16, No. 4, pp. 545-550, July. 2001.

[17] N., Celanovic, D., Boroyevich, "A fast space–vector modulation algorithm for multilevel three–phase converters", IEEE Transactions on Industry Applications, Vol. 37, No. 2, pp. 637–641, March/April 2001.

[18] L., Chengwu, Z., Xiaomin, J., Qiguang, "Research on SVPWM inverter output control technology", Fifth Conference on Measuring Technology and Mechatronics Automation, pp. 927-929, 2013.

[19] A.K., Gupta, A.M., Khambadkone, "A space vector modulation scheme to reduce common mode voltage for cascaded multilevel inverters", IEEE Trans. Power Electronic, Vol. 22, No. 5, pp. 1672–1681, Sep. 2007.

[20] S.K., Mondal, B.K., Bose, V., Oleschuk, J.O.P., Pinto, "Space vector pulse width modulation of three-level inverter extending operation into overmodulation region", IEEE Trans. on Power Electronics, Vol.18, pp.604 – 611, March 2003.

[21] O., Aydogmus,"Design of a solar motor drive system fed by a direct-connected photovoltaic array", Advances in Electrical and Computer Engineering, Vol.12, n. 3, pp. 53-58, 2012.

[22] Y.-H., Lee, B.-S., Suh, C.-H., Choi, D.-S., Hyun, "A new neutral point current control for a 3-level

converter inverter pair system", Industry Applications Conference, Thirty-Fourth IAS Annual Meeting, Vol.3, pp. 1528-1534, 1999.

[23] G., Shiny, M.R., Baiju, "A low computation space vector pwm scheme for multilevel inverters based on fractal approach", IEEE Symposium on Industrial Electronics & Applications (ISIEA), pp. 131–136, 2010.

[24] S.N., Rao, D.V.A., Kumar, C.S., Babu, "New multilevel inverter topology with reduced number of switches using advanced modulation strategies", 2013 International Conference on Power, Energy and Control (ICPEC), pp. 693-699, 2013.

[25] K., Jinsong, C., Yu, W., Haifeng, N., Yichuan, "Three-level inverter speed sensorless system with field orientation control", 2012 IEEE 7th International Power Electronics and Motion Control Conference - ECCE Asia, June 2-5, Harbin, China, 2012.

New Technologies for Modelling in Agricultural Engineering Education

Funda DOKMEN[1]
Zafer ASLAN[2]

Abstract

In recent years, education of agricultural engineering as a renewal structure has been taught as "education of biosystem" in developed countries."Education of Biosystem" which is a branch of engineering that includes the application of biological systems and processes as it extends to engineering science. It is related to agricultural engineering and its fields of study are: "agricultural automation and new developing technologies", "sensitive agriculture techniques", "sustainable agriculture against to changes of climate", "determine of suitable agriculture techniques for global warming and climate changes, and "computer programs and applications of modeling". These subjects include intensive study in the education process. Turkey countinues adopting to educational infrastructures in conformity to developed countries and renewing fast developments in leading agricultural techniques and biotechnology science. In this paper, computer programs and modeling were discussed using the educational process and renewal structure of highschools/vocational schools with the education of the faculty. In addition, teaching of advanced technologies and new trends were examined in terms of globalization and adaptation of mobility based on graduate level of higher education.

Keywords: *Agricultural education, biosystem engineering, higher education, modelling, sensitive techniques*

1. Introduction

In agricultural production, the producers need certain information. This information is closely related with application of modern agricultural techniques and the latest technologies of Biosystem Engineering.

In Turkey approximately 35% of total population work in agriculture sector [1]. Therefore, advanced information should be offered to the producers using computer technology. This is only possible with education reforms which renew itself according to the developing technology. Biosystem Engineering is structured to serve at this point by responding to the needs in agricultural education. Precision Farming is given as one example of the many ways to support agricultural production through high technology, with the aim of reducing energy input, maintaining excellent soil conditions and enhancing yield [2].

At the 'World Forum on Education, Research and Innovation' which was held in Trieste (Italy) in 2007, the roles of space on environmental challenges were discussed by [3]. Morsillo summarizes topics under three items: **i)** Space and the triangle of knowledge; space and technological innovation, research and education, it's role on global responses today's environmental challenges; **ii)** Science and technology supports in environment and climate change, space – based earth observation and monitoring of climate change from space, inter-agency co-operations, contributions to earth observation applications, increasing of integration and synergies, **iii)** Education and investment in Science, Engineering and Technology (SET), Role of careers on knowledge-based society and understanding our planet, education programs and creative learning opportunities of our environments, projects to inspire and motivate students.

A mathematical model is a description of a system using mathematical concepts and language. The process of developing a mathematical model is termed mathematical modelling. Mathematical models are used not only in the natural sciences (such as physics, biology, earth science, meteorology) and engineering disciplines (e.g. computer science, artificial intelligence), but also in the social sciences (such as economics, psychology, sociology and political science); physicists, engineers, statisticians, operations research analysts and economists use mathematical models most extensively. A model may help to explain a system and to study the effects of different components, and to make predictions about behaviour. In the world, where science, economy and professions became globalized, the profession of "Agricultural Engineering" in Turkey should have a certain "International" equivalent among the professions in the world. In this context, considering the applications in European Union (EU) and particularly in United States (USA) which have a leading role in science and technology and the conditions in Turkey; a comprehensive structuralization whose basic principles will remain unchanged should be developed [4,5].

In this paper, computer programs and modeling were examined using the educational process and renewal structure of highschools, then compared with the education of the faculty. The next part of the paper covers explenation for agricultural engineering.

2. Definition of Biosystem Engineering

Biological Systems Engineering is a discipline based on engineering priciples with emphasis on the production and processing of food, fibers, and materials of biological origin. The program is accredited by the Accreditation Board for Engineering and Technology (ABET) [6]. Agricultural and biological engineering embraces a variety of specialty. As new technology and information emerge, specialty areas are created, and many overlap with one or more other areas.

Many students are unaware of Biological Engineering as a discipline, and may wonder what we do. Biological systems engineers design, manage, and develop system and equipment that produce, package, process, and distribute the world's food and fiber supplies.

The United State of America is the first country that started and most commonly applied for the education of Biosystems Engineering at the graduate level. Biosystem Engineering is a new research area for Europe as a scientific concept. Especially, studies countinue for creating learning programmes which are compatible to the practices of Europe Credit Transfer System (ECTS) at the Agricultural Engineering in European Union Countries. Ireland is a leader at the education of Biosystem Engineering in European Union Countries.The education of Biosystem Engineering is taugh at a graduate level in the University of Dublin College in Ireland. This educational term takes four years for the graduate level.The University of Bozok-Yozgat, Uludağ University-Bursa, Sütçü İmam University-Kahramanmaraş and Gaziosmanpaşa University-Tokat were completed studies of adaptation at the education of Biosystem Engineering in Turkey. And also, they are role models for this process.For example; The Universiyty of Uludağ have got one year-prepearing term and four years-graduate courses for Biosystem Engineering.As total, educational terms are five years-graduate courses.

Interesting Focuses of Biosystem Engineering [7] :
- Automation and newly developed technologies in agriculture
- Agricultural machines
- Techniques of modeling and simulation
- Technologies in vegetal/plant and animal production
- Sensitive agricultural techniques
- Post-harvest mechanization applications
- Management and using of land and water sources
- Agricultural structures and environment
- Sustainability and development of rural areas

Work Areas of Biosystem Engineering:
- Govermental sector
- Agricultural machine industry

➢ Machine industry of food and animal production
➢ Company of agricultural consultant
➢ Design office of irrigation and drainage
➢ Countruction firms of agricultural building
➢ Agricultural international trade

3. Modelling and New Technologies

New Technologies and Adaptation of Trends of Modelling in Education of Biosystem and Agricultural Engineering are summarized in this section.

Surface Modelling: EMS-I specializes in hydrologic and hydraulic modeling of watersheds and rivers using the most comprehensive watershed analysis system:The Watershed Modeling System (WMS software) (Fig. 1) is a comprehensive graphical modeling environment for all phases of watershed hydrology and hydraulics. WMS includes powerful tools to automate modeling processes such as automated basin delineation, geometric parameter calculations, GIS overlay computations (cloud nucleous, rainfall depth, roughness coefficients, etc.), cross-section extraction from terrain data, and many more! With the release of WMS 7, the software now supports hydrologic modeling with HEC-1 (HEC-HMS), TR-20, TR-55, Rational Method, NFF, MODRAT, and HSPF [8].
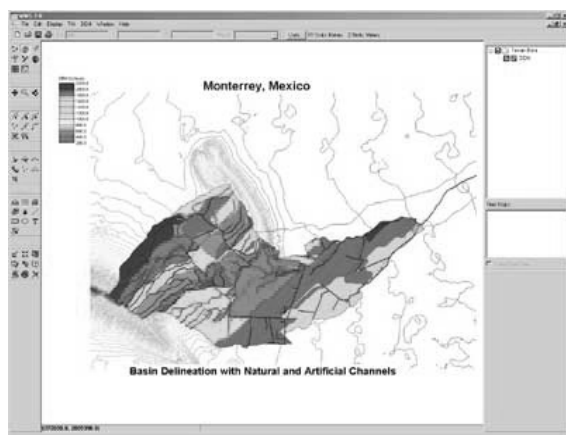
Figure. 1. Surface Modelling: The Watershed Modelling System (WMS)

Dijital Elevation Model (DEM): A digital elevation model (DEM) is a digital representation of ground surface topography or terrain. It is also widely known as a digital terrain model **(DTM).** A DEM can be represented as a raster (a grid of squares) or as a triangular irregular network. DEMs are commonly built using remote sensing techniques, but they may also be built from land surveying. DEMs are used often in geographic information systems, and are the most common basis for digitally-produced relief maps [9]. Digital Elevation Model (DEM) can be defined as a model which expresses the topography of the earth in its simplest form, three-dimensionally using X, Y planimetric and Z elevation values. Figure 2 indicates an example of Digital Elevation Model.
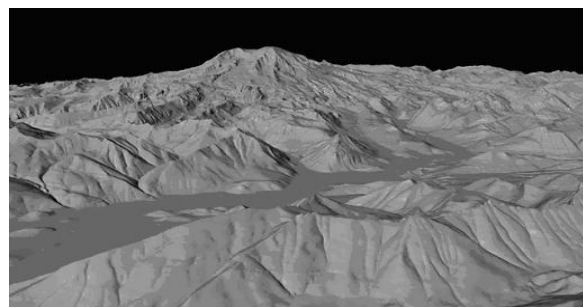
Figure 2. Digital Elevation Model (DEM)

Digital Terrain Models (DTM): DTM includes details with different elevation values on topography such as buildings, flora, forest etc and reflects the visible topography. In this course the students will learn mathematical bases of digital terrain models and digital surface models based on 3 dimensional coordinate data. They will also learn mathematical basis of different filtering and collocation calculation methods which are used in professional stabilizing calculation. They will learn mathematical and methodological information about interpolation techniques used in formation of digital terrain and surface models. In practice, among a range of digital calculation programs, digital calculations in Microsoft Excel and Golden Surfer software and method will be taught to the students [10].

Wavelet (Mathematical Model):A wavelet is a wave-like oscillation with an amplitude that starts out at zero, increases, and then decreases back to zero. It

can typically be visualized as a "brief oscillation" like one might see recorded by a seismograph or heart monitor. Generally, wavelets are purposefully crafted to have specific properties that make them useful for signal processing. Wavelets can be combined, using a "shift, multiply and sum" technique called convolution, with portions of an unknown signal to extract information from the unknown signal. Figure 3 indicates an example wavelet signals [11]. Interpretation of 1D Countinuous Wavelet and 1D Wavelet Packets explain small, meso and large scale influences on agricultural productions [12].
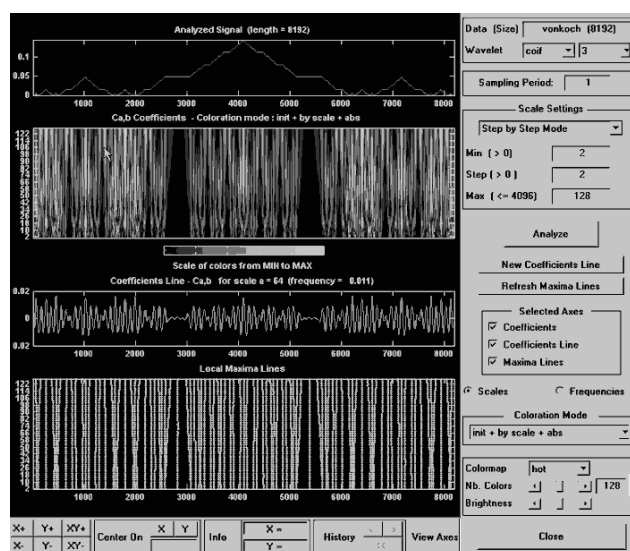
Figure 3. Wavelet Signals

Matlab: It is a high-level technical computing language and interactive environment for algorithm development, data visualization, data analysis, and numeric computation [13]. Using the Matlab product, you can solve technical computing problems faster than with traditional programming languages, such as C, C++, and Fortran.You can use Matlab in a wide range of applications, including signal and image processing, communications, control design, test and measurement, financial modeling and analysis, and computational biology. Add-on toolboxes (collections of special-purpose Matlab functions, available separately) extend the Matlab environment to solve particular classes of problems in these application areas (Fig. 4). Matlab provides a number of features for documenting and sharing your work. You can

integrate your Matlab code with other languages and applications, and distribute your Matlab algorithms and applications [14].
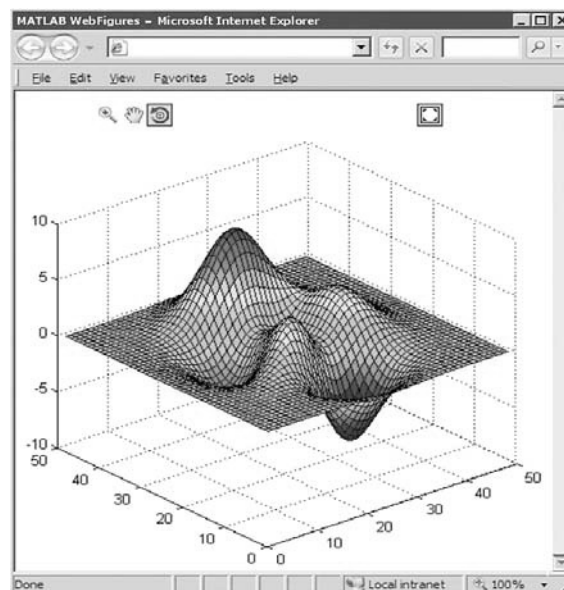
Figure 4. Applications of Matlab

SWS: SWS has been developed by USDA-ARS E. Brown Jr. Salinity Laboratory. SWS performs simulations on water and soil chemistry.The model takes in to account the carbonate chemistry very precisionally which is very important for alkalinity and salinity simulations and this particularity makes the SWS distinctive among the other model [15]. This model was developed to evaluate the appropriateness of the quality of the irrigation water, salinity and the qualities of alkalinity particularly in arid and semi-arid regions.

GIS: The definition of Geographic Information Systems, the properties of raster and vector data, preparation of soil maps and digital soil maps in data bases, the role of GIS in sustainable use of natural sources, the use of digital soil data in pollution and erosion model studies, advanced GIS software such as CBS, Arc View, Arc Info, Grass Land are used in management of soil and water sources [10].

Landsat: The Landsat Program is the longest running enterprise for acqusition of imagery of the earth from space. The instruments on the Landsat satellites have

acquired millions of images. The images, archived in the United States and at Landsat receiving stations around the world, are a unique resource for global change research and applications in agriculture, geology, forestry, regional planning, education and national security (Fig. 5.), [16].
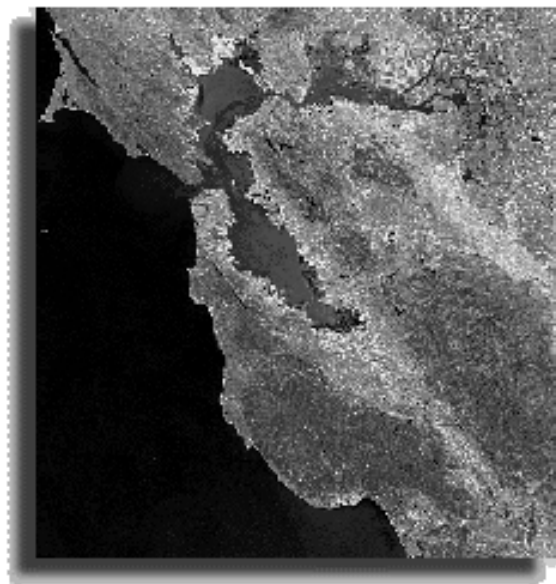
Figure 5. Landsat Thematic Mapper image of the San Francisco Bay Area (sampled): 60 kbytes

RUSLE (Water Erosion Estimation Models): They are used in studies on the importance of water erosion, the history of soil loss estimation equations, soil loss tolerance, revised universal soil loss equation and factors values.

Mathematical Models in Irrigation and Drainage: They are used in researches and various mathematical models [10].

Irrigation Programming Techniques: Different irrigation programming methods and techniques are used according to irrigation methods.

SALT-MOD: SaltMod is a mathematical, numerical computer program for the simulation and prediction of the salinity of soil moisture, ground and drainage water, the depth of the watertable (water table), drain discharge and leaching of salts in irrigated agricultural lands under different geohydrologic conditions,

varying water management options, including the (re)use of groundwater for irrigation by pumping from wells (conjunctive use), and several crop rotation schedules.It uses salt and waterbalances. The model aims at sustainable land use and environmentally sound optimal water management for sustainability and can be used for the reclamation (remediation, rehabilitation, restoration) of saline soils [17].

Fuzzy-Logic: Fuzzy logic is a form of multi-valued logic derived from fuzzy set theory to deal with reasoning that is approximate rather than precise. In contrast with "crisp logic", where binary sets have binary logic, the fuzzy logic variables may have a membership value of not only 0 or 1 – that is, the degree of truth of a statement can range between 0 and 1 and is not constrained to the two truth values of classic propositional logic [18]. Fuzzy logic emerged as a consequence of the 1965 proposal of fuzzy set theory by Lotfi Zadeh [19, 20]. Furthermore, when linguistic variables are used, these degrees may be managed by specific functions. Figure 6 shows a Fuzzy Logic System [21].
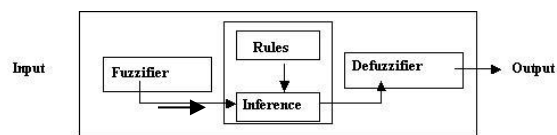
Figure 6. A Fuzzy Logic System

Numerical Experiments: Numerical model was setup using three nested grids using (45x55), (70x91), and (79x142) grid points in (north-south x west-east) directions using 108, 36, and 12 km horizontal grid spacing, respectively (Fig. 7). MM5 was configured using simple ice microphysics for the treatment of excess moisture, cumulus to parameterization of convective motions, boundary layer to resolve the atmospheric flow within the boundary layer, Rapid Radiative Transfer Model (RRTM) for calculation of radiation and 5-layer soil model for the calculation of surface fluxes [22].
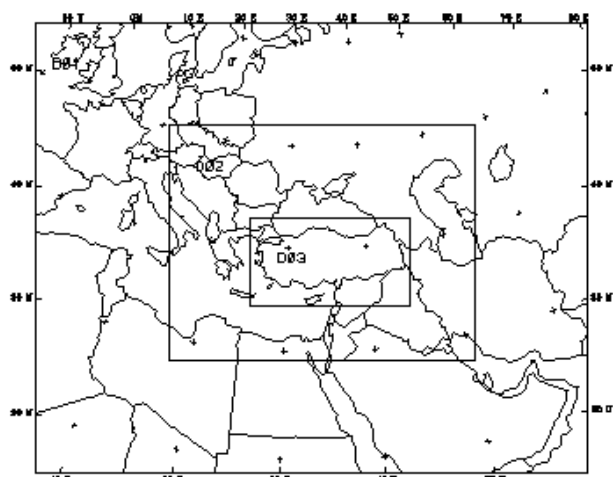
Figure 7. The setup of the three nested grids

NCAR's next generation non-hydrostatic mesoscale model, Advanced Research WRF (WRF-ARW) are used to analyse complex topography and variableclimate conditions [23].

ICTP-RegCM3 model that is based on MM5, the predecessor of WRF.WRF on the other hand, is superior to RegCM and MM5 in both physics, dynamics and numerics, but computationally more expensive accordingly. However, WRF is still under development and requires more performance analyses for its validation in regional climate modelling.

CORINE soil erosion assessment methodology the following maps would be prepared; Land use maps, aspect maps, slope maps,topographic maps,land cover maps, soil erodibility maps [24].

3. Results

When advanced technologies and new modeling trends take place at the graduate level, these processes will help globalization of biosystem education. Besides, adaptation will be easier for international student exchange.

Adaptation Process at the Education of Biosystem Engineering

1. Decision theory should be developed for education
2. Decision-support alternatives should be determined
3. Education strategies should be set out
4. Every country should consider its won educational facts and determined their requirements
5. Potential production must determine according to ecological characteristics of country
6. Using of modern and advance technologies take place to the education of agricultural (Exp: monitoring, controlling, automotion, mechanization, fertilizer, fumigation, harvesting, irrigation, packing house etc.,).

Advantages of adaptation in biosystem engineering are:

1. Integration with the world is achieved
2. Student profile and quality increased
3. The students prefer "Biosystem Engineering" consciously and upon their will
4. Adaptation of globalization and changing is easier at the education of agricultural
5. To help common and sustainable agricultural education according to global changing of climate
6. To focused in the constituents of international agricultural education
7. To increase the quality of education to be able to compete in agricultural education in national and international level
8. Accreditation of the courses and diplomas is completed the level of international and global
9. Integration of evaluation of diploma and titles of the participants from other countries prior to masters or doctorate programs with re-structuralization

Training: A Case Study

- Short courses for students, post-graduates etc. on specific research issues should be organised,
- One international workshop has to be organised, which will manage the workshops directly with the partner or group of partners involved.

Working programs (WP1-3) and Logical Frame Works would be listed as below (Table 1):

Table 1. Details on working programs for developing curriculum (sample for work packets)

WP1	Project web site: Portal connection to project Dbases and external links
	1st International Workshop
	Coordination of the WGs activities: WGs meetings
	COORDINATION PLENAREY meetings
	Coordination of the information network between the ECVET partners
WP2	Data bases of: training programs complete case studies
	Training activities and short courses
	Exchanges of researchers, short-term visits, etc
WP3	Collection of existing programs
	Validation of new programs with case studies applications
	Development curriculum
	Development of guidelines for curriculum studies.

4. Conclusion

"Education of Agricultural Engineering" which is a branch of engineering that includes the application of biological systems and processes as it extends to engineering science. It is related to agricultural engineering and its fields of study are: "agricultural automation and new developing technologies", "sensitive agriculture techniques", and "computer programs and applications of modeling". These subjects include intensive study in the education process.

Nowadays, advanced technologies uses are increasing everyday. However, in the world of globalization technologies re-structural changing and adaptation of international norms are necessary in the education of agricultural. In the respect that techniques of modeling and simulation take place at the graduate and vocational level of universities during the teaching processes. During the educational process, these techniques support for student's thesis, projects and their homework. So, students will be able to practice in relation to their technical course.

REFERENCES

[1] Cevheri, C.İ. (2004). Tarımsal Bilişim ve GAP (Agricultural Informatics and South Anatolia Project) (Harran Üniversitesi, Akçakale MYO), Tarımsal Bilişim Teknolojileri 4. Sempozyum Bildiriler Kitabı, Türkiye.

[2] Ammann, K. (2008): "Feature: integrated farming: why organic farmers should use transgenic crops", New Biotechnol. 25, p. 101–107.

[3] Morsillo, G., (2007), "Environment: Global Challenges, the Role of Space", G8 UNESCO World Forum on Education, Research and Innovation, May 10-12, 2007, Triese, Italy.

[4] Anonymous (2008a). Biyosistem Mühendisliği Lisans Programı (The Programme of Biosystem Engineering), Başvuru Dosyası, T.C. Uludağ Üniversitesi, Ziraat Fakültesi, s:321, Bursa, Türkiye.

[5] Anonymous(2009).http://www20.uludag.edu.tr/~tys/biyosistem/sitemapl.htm (**Date:30.12.2009**)

[6] Anonymous (2011a). http://www.bse.wisc.edu (**Date: 30.03.2011**)

[7] Anonymous (2011b).http://bse.bozok.edu.tr (**Date:17.03.2011**)

[8] Anonymous (2010a).http://www.xpsoftware.com/products/watershed. modeling-system-wms/ (**Date: 10.01.2010**)

[9] Anonymous(2010b).http://en.vikipedia.org/wiki/Digital_elevation_model(**Date: 10.01.2010**)

[10] Dökmen, F. and Duru, N. (2010). Trends of Modeling or Computer Systems in Education of Biosystem, Biotech 2010, The Moscow International Conference 'Biotechnology: Ecology of Big Cities', Biotechnology and

Ecology 2010, Abstract Book, p: 379, Moscow, Rusia.

[11] Anonymous (2010c).http://mathsworks.com/products/wavelet/, Wavelet Toolbox 4.5, Analyze and Synthesize Signals and Images Using Wavelet Techniques (**Date: 15.01.2010**)

[12] Dökmen, F. and Aslan, Z. (2013). Evaluation of the Parameters of Water Quality with Wavelet Techniques, *Water Resources Management*, DOI: 10.1007/S11269-013-0454-5, 27:4977-4988, Springer.

[13] Anonymous (2010d). http://www.mathworks.com (**Date: 15.01.2010**)

[14] Anonymous (2010e). http://www.mathworks.cn/products/netbuilder/ (**Date: 15.01.2010**)

[15] Kesmez, G.D., Suarez, D.L., Taber, P. (2008). SWS (Soil-Water-Salinity): Doymamış Koşulda Çözelti Transferi Modeli (Solution Transfer Model in Unsaturated Condition), s:197-216, Sulama Tuzlanma Toplantısı, 12-13 Haziran, Şanlıurfa Türkiye.

[16] Anonymous (2010f). Geo.arc.nasa.gov/sge/landsat/landsat.html (**Date: 10.01.2010**)

[17] Anonymous (2008b).http://www.waterlog.info/saltmod.htm

[18] Novák, V., Perfilieva, I., and Močkoř, J. (1999). Mathematical Principles of Fuzzy Logic Dodrecht: Kluwer Academic. ISBN 0-7923-8595-0

[19] Anonymous (2006). "Fuzzy Logic". Stanford Encyclopedia of Philosopy. Stanford University. 2006-07-23. Retrieved 2008-09-29.

[20] Zadeh, L.A. (1965). Fuzzy Sets, Inform Control 8:338-353.

[21] Duru, N., Dökmen, F., Canbay, M.M., and Kurtuluş, C. (2010). Soil Productivity Analysis Based on A Fuzzy Logic System, *Journal of the Science of Food and Agriculture*, DOI:10.1002/jsfa.4074, Online ISSN: 1097-0010, Vol.90 (3), ISSN:0022-5142, p:2220-2227, WILEY InterScience.

[22] Gürer, K, 2010. Model Performance Evaluation of MM5 Model Initialized using CCSM3 Data for Future Air Quality Studies, California Air Resources Board, Technical Document.

[23] NCAR (2011). http://doi.ieeecomputersociety.org/10.1109/HPC.1997.592119,(April 3, 2011).

[24] Aslan, Z., D. Gabriels, C. Ayday, G. Erpul, K. Gürer, N.Yeniçeri, S. Söğüt, B. Oğuzhan, D.Okçu, N.Çağlar, A. Tokgozlu, (2010). "Actual Erosivity Analysis based on Ground Measurements and Remote Sensing Data", TUJJB-TUMAHAP-01-06, BU, Turkey.

Cost Estimation Comparisons Between Least Square Regression and Quantile Regression on Fiber Reinforced Bridge Projects

Ankith Reddy PAMULAPARTHY[1]
Robert C. CREESE[2]
Hota V. GANGARAO[3]
Majid JARIDI[4]

Abstract
This paper focuses on the Least Square (LS) regression using the mean and Quantile (M) regression analysis using median which is based on "well-Known" parametric estimation methodologies. Data from Oregon and California highway bridges were used for the comparison of the two methods. Relationships were developed to predict the unit cost of FRP repair work and FRP cost was found to have a high degree of correlation with FRP area for both Oregon and California. It was observed that the Cost Estimating Relationships (CERs) obtained by Quantile (M) regression method had the smaller Mean Absolute Deviation (MAD) values and lower Mean Absolute Percentage Error (MAPE) values than Least Square (LS) regression. The stuudy showed that Quantile Regression is much less sensitive to outliers than Least Squares Regression.

Keywords: *Quantile regression, cost estimating relationships (cers), fiber reinforced polymer (frp) wraps, outliers*

1. Introduction

State transportation departments are faced with a challenge to keep bridges under their jurisdiction in good operating conditions. Corrosion of bridges has been a constant challenge for engineers and new materials (e.g. polymers, metals, ceramics and their composites) are being developed to minimize corrosion related issues. Fiber Reinforced Polymers (FRPs) are composites that combine the strength of fibers with the stability of polymer resins. The strength of FRP materials comes from the type of fibers used, usually they are glass, carbon or aramid fibers. The primary advantages of FRP materials are: lightweight, non-magnetic, high corrosion resistance and high strength to weight ratio. These advantages make FRP materials a viable option for the initial construction or for

rehabilitation of current bridges. As a new technology, it is hampered by a lack of approved standards and an effective cost estimation methodology.

Cost Estimating Relationships (CERs) are the parametric equations that are developed between different variables to determine the cost of a project component or the total cost of the project. These relationships are developed by cost estimators and are used by managers to control the variables that impact the cost of a project [4]. The primary statistical method to develop CERs is Least Square (LS) regression which is based upon the mean of the data. An alternative method is the Quantile (Q) regression which is based upon the median of the data [6]. This project compares

---

[1] *Graduate Student, Industrial and Management Systems Engineering, Benjamin M. Statler College of Engineering and Mineral Resources, West Virginia University, West Virginia, USA, ankith.redde@gmail.com*

[2] *Professor Emeritus, Industrial and Management Systems Engineering, Benjamin M. Statler College of Engineering and Mineral Resources, West Virginia University, West Virginia, USA, Robert.Creese@mail.wvu.edu*

[3] *Professor, Civil and Environmental Engineering Department & Director of the Constructed Facilities Center, Benjamin M. Statler College of Engineering and Mineral Resources, West Virginia University, West Virginia, USA Hota.Gangarao@mail.wvu.edu*

[4] *Professor, Industrial and Management Systems Engineering, Benjamin M. Statler College of Engineering and Mineral Resources, West Virginia University, West Virginia, USA Majid.Jaridi@mail.wvu.edu*

the two methods using limited data on highway rehabilitation projects in Oregon and California utilizing the software ESTIMFEC [1] to perform the analysis. One of the problems of using historical data is that it may contain outliers and Quantile regression is less sensitive to outliers than the Least Square regression.

2. Methodology

Least Square regression is the most commonly used method to develop linear predictive relationships including cost relationships and engineering relationships. Quantile methods are commonly used to determine percentile rankings used on many testing scores and in areas such as finance and sociology. Quantile regression methods have been used within labor or educational economies to study wage determinants, trends in income inequality or effects of socioeconomic characteristics on education attainment [3].

2.1 Least Square (LS) Regression

Least Square regression is a statistical method of analysis that estimates the relationship between one or more independent variables and the dependent variable by minimizing the sum of squares of the difference between the observed and predicted values of the dependent variable [8]. A simple Least Square regression model involving only one independent variable (X) predicting a dependent variable (Y) is expressed by Equation 1.

$$Y = a + bX + \varepsilon \tag{1}$$

Here "a" is the intercept that indicates where the straight line intersects Y–axis; "b" is the slope that indicates the degree of steepness of the straight line and "ε" represents the error. The best line or a relationship would be the one with the Least Sum of Squared Errors (SSE) [9].

$$SSE = \sum (Y_i - \hat{Y})^2 \tag{2}$$

Where

Y_i = Dependent variable i and where i = 1,......n

$$\hat{Y} = (\sum Y_i)/n \tag{3}$$

2.1.1 Drawbacks of Least Square (LS) Regression

According to Foussier [4], the main drawback is "regression". If there are a large number of observations and they are scattered, the Least Square method underestimates the larger observations and overestimates the smaller observations as the Least Square method regresses towards the average value. It is a major drawback, since the costs of a product or project are always scattered, and there is no necessity for the cost to regresses towards the average cost. The Least Squares regression is based upon the data having a normal distribution and this does not always occur. If the data is truly normal, then the mean and median would be the same. The other major disadvantage of the Least Square method is that it is sensitive to outlier that is due to squaring of the error term. Since the Least Square method is not robust, this might have a tremendous impact on the predicted cost. Foussier [4] indicates it is due to the small break down of the arithmetic average. Hence, the change of just one data point might have a severe impact on the predicted cost. The outliers that are far away from the tentative CER will strongly impact the predicted cost and the R^2. A tendency to eliminate the outliers to increase R^2 might cause one to eliminate too many data points.

According to Xia [10], the third disadvantage of Least Square method is multi-collinearity. There may be several variables that may be linearly collinear to each other in the data. It may adversely affect the coefficient of the estimates when there is a small change in the data. The relationship thus obtained between these variables does not make sense even though it is mathematically correct and produces a large confidence interval. This is due to the fact that to estimate the values of the parameters one needs to compute the inverse of the matrix based on the inputs. The determinant of a matrix with two collinear variables is equal to zero and hence these matrices cannot be inverted reliably to estimate the parameters [4]. However the relationships developed in this study were concerned with only one variable.

2.2 Quantile Regression

According to Koenker [6] Quantile Regression is the estimation of Quantiles of the conditional distribution. It models the relation between a set of predictor variables and the specific Quantiles of the response variable. The prominent form of Quantile regression is the Median regression. Koenker and Bassett stated that for a sample $Y_1, Y_2....Y_n$ from a population Y, we can compute the sample median ν by minimizing the sum of absolute deviations.

$$\hat{\nu} = min \sum_{i=1}^{n} |Y_i - \nu| \qquad (4)$$

Similarly we can compute the τth sample Quantile $\nu(\tau)$ by minimizing the absolute deviations of various Quantiles.

$$\hat{\nu}(\tau) = min \sum_{i=1}^{n} \rho_\tau |Y_i - \nu| \qquad (5)$$

Here $\rho_\tau(z) = z(\tau - I(z < 0)), 0 < \tau < 1$. $I(.)$ denotes the Indicator function. Koenker stated that the optimal value of τ is the median. The estimate of linear conditional Quantile function (i.e. of $Q_\tau \left(\frac{Y_i}{X_i}\right) = X_i \beta_\tau$) can be found by the criterion:

$$\hat{\beta}(\tau) = \arg min \sum_{i=1}^{n} \rho_\tau |Y_i - X_i \beta| \qquad (6)$$

Where $\hat{\beta}(\tau)$ is called the τth regression Quantile. The minimizer function $\sum_{i=1}^{n} \rho_\tau |Y_i - X_i \beta|$ is differentiable except at $Y_i = X_i \beta$. A simplex based algorithm was developed by Barrodale and Roberts [2] to solve the minimizer function and was later extended by Koenker and d'Orey [7] to Quantile regression estimation. The case where $\tau = 1/2$ corresponds to median regression, which is also known as L1 regression.

3. Data Source and Analysis

3.1 Oregon Bridges

The state of Oregon had several bridges that have undergone repair and rehabilitation work in recent times. There were seventeen bridges that had undergone repair work using FRP wrappings for which the data was obtained. The area of the bridges ranges from 500 ft^2 to 9,204 ft^2. There were multiple bids that were quoted for each bridge repair work by several contractors. Table 3.1 gives the total contract cost, FRP area, FRP cost and other calculated parameters.

Table 3.1: Summary of Year, Accepted FRP Cost, Accepted FRP Unit Cost and Total Contract of Oregon Highway Bridges

Location	Year	Bridge No.	FRP Area, ft^2	Accepted FRP Unit Cost, \$/ft^2	Accepted FRP Cost, \$	Total Contract, \$	% of FRP Cost of Total Contract
OR	2007	01786A	3,144	50.68	159,343	12,537,779	1.27
	2008	07601B	712	40.82	29,062	2,548,552	1.14
	2008	08381S	1,280	39.30	50,299	2,548,552	1.97
	2008	7458	1,955	97.20	190,020	10,193,994	1.86
	2008	08383N	6,103	27.47	167,665	3,324,179	5.04
	2009	8843	2,345	106.82	250,480	3,442,437	7.28
	2009	03173A	9,204	13.48	124,069	3,885,033	3.19
	2010	7530	500	61.11	30,557	2,002,807	1.53
	2010	7532	500	61.11	30,557	2,002,807	1.53
	2010	7533	500	13.10	6,548	2,002,807	0.33
	2010	7534	500	61.11	30,557	2,002,807	1.53
	2010	06945A	840	38.98	32,739	3,013,112	1.09
	2010	04981A	1,900	31.59	60,022	976,687	6.15
	2010	02233A	1,900	40.20	76,391	976,687	7.82
	2010	04979A	2,600	27.70	72,026	976,687	7.37
	2010	02236A	3,200	27.28	87,304	976,687	8.94
	2010	7392	5,800	30.11	174,609	457,704	38.15

Note: All the cost data has been adjusted for inflation to 2013 dollar value

The accepted FRP cost and FRP area are the two variables that are used to predict the unit cost of FRP repair work. The total FRP cost constitutes a minor fraction of the total contract cost. Hence during the estimation of unit cost of FRP repair work, FRP cost is used instead of the total contract cost. Only one layer of FRP application was considered due to limited availability of the data. Bridges with accepted FRP cost of less than 1% of the total contract cost were omitted from the paper. Bridge No. 7533 was found to have a value of 0.33% (Table 3.1) and was not considered in the study as its cost was more than 70 percent lower than three other bridges with the exact same area. Figure 3.1 shows the scatter plot of FRP cost and FRP area. Figure 3.1 indicates three points (i.e. bridges 7458, 8843, 03173A) to be potential outliers. The R^2 value obtained for all the data points included is 0.278 and coefficient of determination (R^*) value obtained for Quantile (Median) regression is 0.430. The bridge 01786A was not considered to be an outlier since its FRP cost was within 95% of the confidence interval and no physical characteristic was detected that indicated it to be an outlier.

It can be observed from Figure 3.1 that the Least Square regression method overestimated smaller values and underestimated larger values when compared to Quantile (Median) regression. The slope of the two equations are different and the Least Squares is greatly affected by the outliers as indicated by Equations 7 and 8. The regression equations obtained by Least Sqaure and Quantile (Median) methods for all the data included are:

Accepted FRP Cost (LS-$) =57,515 + 15.19*FRP Area(ft^2)   (7)

Accepted FRP Cost(Q (M)-$) =18,321 + 24.47*FRP Are(ft^2)   (8)

The coefficient of determination values obtained are 0.278 (LS, R^2) and 0.430 (Q (M), R^*) respectively. The equations have very different slopes and some of the data points appear as outliers. When the outliers are detected and removed, the two methods will be in more agreement.

Further analysis for outliers is made by conducting a Tietjen-Moore Test for multiple outlier detections. The number of suspected outliers in the test were considered to be three (i.e. k = 3). The value of test static E^k to be 0.2131 which is less than the critical value of 0.2249 thus confirming the presence of three outliers in the data. When the number of suspected outliers in the test were considered to be four (i.e. k = 4) the test static (E^k) value (0.1910) was greater than the critical value (0.1508) and did not confirm four outliers. Further residual analysis wais carried out to identify these outliers.
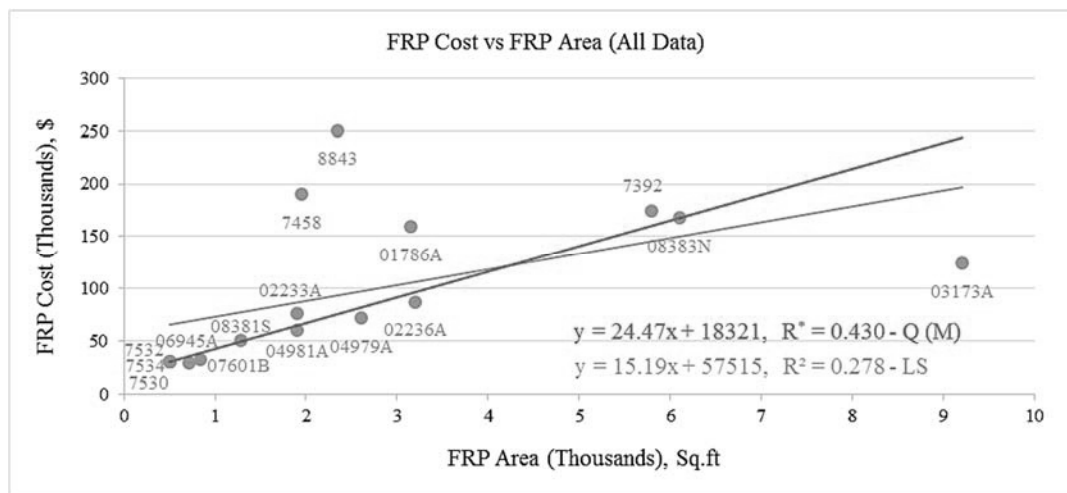

Figure. 3.1: Scatter Plot (All Data) of Accepted FRP Cost and FRP Area of Oregon Highway Bridges (Q (M)) & LS) with R^2 = 0.278 & R^* = 0.430

The computations to identify the outliers are made in three steps:

1. A linear relationship is obtained using all the data points and the prediction of FRP cost for each bridge is made using this relationship. Deviations of the predicted FRP cost from the actual FRP cost is computed as "Deviations 1".

2. Then each data point is successively discarded and therefore N new relationships are computed. Appendix 1 shows the R^2 corresponding to the new relationship without this data point and the deviation, called "Deviation 2" between this data point and the new relationship. A few R^2 are much higher (>0.100) than the corresponding data points are identified as outliers since their deletion greatly improves the relationship.

3. The difference between both the deviations is divided by the standard deviation of "Deviation 1" and is multiplied by a factor of 100. The column "Relative Variation" from Appendix 1 gives the resultant value. The data points that have a relative variation of more than ±50% are considered to be outliers in this paper.

Appendix 1 shows that bridges 7458 and 03173A had a relative variation more than the threshold value of ±50% thus indicating them to be possible outliers. Appendix 2 also shows that removing the bridge 8843 greatly improves the correlation between the FRP cost and FRP area.

➢ Bridge 03173A is a seismic retrofit involving different repair procedure than the rest of the bridges thus having a much higher cost than the rest of the bridges.

➢ Bridge 7458 involved construction and removal of various temporary work platforms with enclosure. The humidity and temperature in the enclosure was maintained using an HVAC system which is the likely reason for higher unit cost of FRP repair work.

➢ Bridge 8843 has many elements that contain asbestos. The contractor had to remove these

materials before proceeding with the FRP application.

Bridges 03173A, 7458 and 8843 were identified as spurious bids considering their unusual FRP repair cost. These bridges were considered as outliers and were not considered in further analysis of the data.

Equation 9 was obtained for accepted FRP cost against FRP area for all the bridges in Oregon by Least Square method with an R^2 of 0.884 is given by:
Accepted FRP Cost (LS-$) =16,736 + 27.03*FRP Area (ft^2) (9)

Equation 10 was obtained by performing Quantile (Median) regression for accepted FRP cost against the FRP repair area for all the bridges in Oregon with an R^* value of 0.773 is given by:

Accepted FRP Cost (Q (M)-$) = 18,321 + 24.47*FRP Area (ft^2) (10)

The intercept values (16,736 (LS), 18,321 (Q (M))) represent the fixed set-up costs such as mobilization, equipment and traffic control.

Figure 3.2 is developed between the accepted FRP cost against FRP area to compare the two methods (LS & Q (M)) of analysis. It shows the extreme observation point (01786A) had minimal impact on the relationship obtained by Quantile (Median) regression method. The slope difference (absolute) between the CERs of Figure 3.1 and Figure 3.2 is 0 (Q (M)) and 11.84 (LS) which indicates the robustness of Q (M) regression with respect to outliers. The slope of CER obtained by Least Square method changed more than 75% indicating a high influence of outlier on the Least Square method whereas the outliers has no effect on the CER obtained by the Qunatile method. When the outliers are removed, agreement is high as indicated by Figure 3.2.

The results from Table 3.2 show that Least Square regression method has the least SSE value and Quantile (Median) regression method has the least MAD and MAPE values. Profits and costs are indicated better by the mean absolute deviation and by the mean absolute

percentage error than by the sum of squares of the errors. A relationship between the accepted FRP cost and the FRP area to predict the unit cost ($/ft^2) values, can be established. The predicted unit cost obtained from Equations 11 and 12 are given by:

Unit Cost (LS-$/ft^2) = 27.03 + 16,736/FRP Area (ft^2) (11)

Unit Cost (Q (M)-$/ft^2) = 24.47 + 18,321/FRP Area (ft^2) (12)
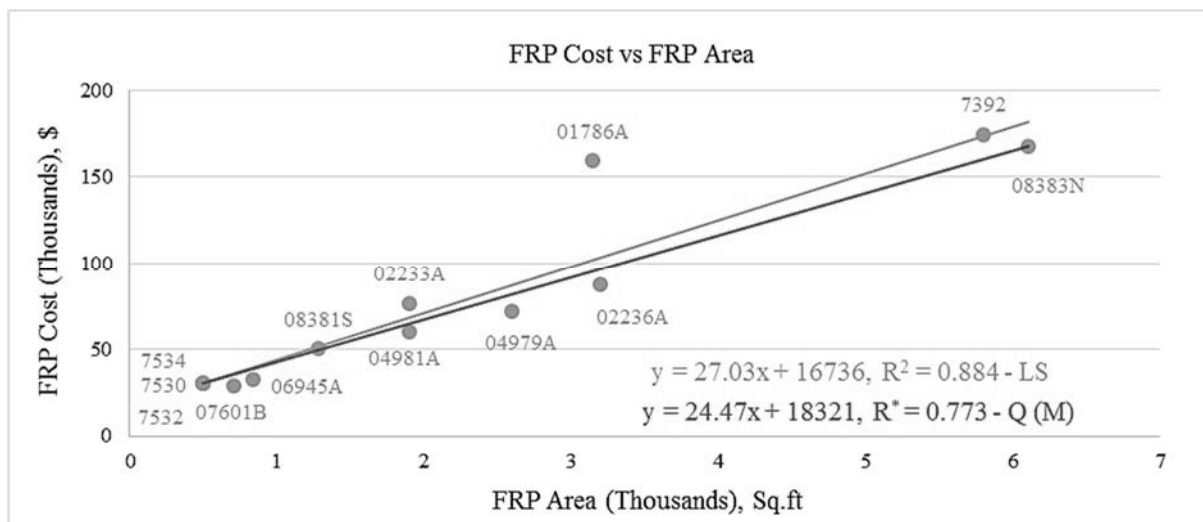
Figure. 3.2: Scatter Plot of Accepted FRP Cost and FRP Area of Oregon Highway Bridges (LS & Q (M)) with R^2 = 0.884 & R* = 0.773

Table 3.3 shows the predicted FRP unit cost ($/ft^2) values obtained by the two methods (LS & Q (M)) of analysis using Equations 11 and 12.. These equations are similar as the outliers have been determined and removed, and thus agreement between the two methods is high. The actual unit costs versus predicted unit costs have good agreement overall, but the predicted equations are approximate only. There is the assumption that the start-up costs, which is indicated by the intercept of the curve, is constant for all project sizes. When the bridges are grouped into two ranges as done in Table 3.3, the agreement is much better for the unit costs.

Table 3.4 gives the weighted average by area of FRP unit cost for the two different methods of analysis for two separate area ranges (i.e. <2000 & >2000). The weighted average values for both the Quantile method and the Least Squares method are near the actual unit cost values. The difference in values between the two area ranges indicate the large impact of area upon FRP unit cost

Table 3.2: Residual Analysis Table for Oregon Highway Bridges

Area, ft^2	Accepted FRP Cost, $	Predicted FRP Cost, $		SSE (X-Xp)^2	
		Least Square	Quantile (Median)	Least Square	Quantile (Median)
712	29,062	35,989	35,744	47,981,936	44,646,310
1,280	50,299	51,347	49,643	1,097,351	431,329
6,103	167,665	181,756	167,661	198,569,710	10
500	30,557	30,256	30,556	90,024	0
500	30,557	30,256	30,556	90,024	0

500	30,557	30,256	30,556	90,024	0
840	32,739	39,450	38,876	45,032,308	37,658,713
1,900	60,022	68,111	64,814	65,437,468	22,965,764
1,900	76,391	68,111	64,814	68,562,082	134,033,976
3,144	159,343	101,748	95,255	3,317,230,332	4,107,312,760
2,600	72,026	87,038	81,943	225,369,002	98,345,164
3,200	87,304	103,262	96,625	254,639,705	86,874,557
5,800	174,609	173,563	160,247	1,093,099	206,258,302
Total	1,001,130	1,001,144	947,289	4,225,283,064	4,738,526,887

MAD				MAPE, %	
Area (ft^2)	Least Square	Quantile (Median)		Least Square	Quantile (Median)
712	6,927	6,682		23.84	22.99
1280	1,048	657		2.08	1.31
6103	14,091	3		8.4	0
500	300	1		0.98	0
500	300	1		0.98	0
500	300	1		0.98	0
840	6,711	6,137		20.50	18.74
1,900	8,089	4,792		13.48	7.98
1,900	8,280	11,577		10.84	15.16
3,144	57,595	64,088		36.15	40.22
2,600	15,012	9,917		20.84	13.77
3,200	15,957	9,321		18.28	10.68
5,800	1,046	14,362		0.60	8.23
Average	10,435	9,811	**Average**	12.15	10.70

Table 3.3: Summary of FRP Repair Unit Cost ($/Ft^2) Obtained For Oregon Highway Bridges

FRP Area, ft^2	Actual FRP Cost, $	Actual FRP Unit Cost, $/ft^2	Pred. FRP Unit Cost (LS), $/ft^2	Pred. FRP Unit Cost (Q (M)), $/ft^2
712	29,062	40.82	50.55	50.20
1,280	50,299	39.30	40.11	38.78
6,103	167,665	27.47	29.78	27.47
500	30,557	61.11	60.51	61.11
500	30,557	61.11	60.51	61.11
500	30,557	61.11	60.51	61.11
840	32,739	38.98	46.96	46.28
1,900	60,022	31.59	35.85	34.11
1,900	76,391	40.21	35.85	34.11
3,144	159,343	50.68	32.36	30.30
2,600	72,026	27.70	33.48	31.52
3,200	87,304	27.28	32.27	30.20
5,800	174,609	30.10	29.92	27.63

Table 3.4: Summary of Average FRP Unit Cost ($/Ft^2) Obtained For Respective Area Range of Oregon Bridges

FRP Area Range, ft^2	Average* FRP Unit Cost, $/ft^2 (LS)	Average* FRP Unit Cost, $/ft^2 (Q (M))	Average* FRP Unit Cost, $/ft^2 (Actual)
<2000 (8)	43.50	42.49	41.83
>2000 (5)	31.05	28.87	31.70

*The area of the respective bridges was considered as weight in calculating the average FRP unit cost

3.2 California

There were a total of seven bridges (Table 3.5) for which the contract data was obtained which had undergone FRP repair and rehabilitation work in California. These bridges were spread across Alameda County, Santa Barbara County, Tulare County, Los Angeles County, San Bernardino County, Riverside County and Imperial County. There were multiple contract bids for each bridge. Table 3.5 gives the Contract number, FRP cost, FRP area, Total contract cost and other calculated parameters.

Table 3.5: Summary of Year, Accepted FRP Cost and Accepted Unit Cost for California Highway Bridges

Location	Contract No.	Date	Area, ft^2	Accepted Unit Cost, $/ft^2	Accepted FRP Cost, $	Total Contract, $	%FRP Cost
	06-0N8504	2012	170	98.61	16,763	735,961	2.28%
	11-264004	2010	420	84.40	35,449	995,644	3.56%
	08-472304	2008	614	62.01	38,075	39,726,300	0.10%
CA	10-0W0704	2012	2,620	70.81	183,974	2,559,279	7.19%
	08-0G4804	2011	3,375	95.00	320,625	1,482,509	21.63%
	06-0C1304	2012	3,677	65.29	238,053	3,352,320	7.10%
	08-0M94U4	2012	4163	60.12	248,157	24,155,220	1.03%

Note: All the data has been adjusted for inflation to 2013 dollar values

The California bridge data (Table 3.5) was mainly categorized into FRP repair work. FRP area is the variable which was found to have a significant correlation with the total FRP cost. The regression equations obtained by Least Square and Quantile (Median) methods for all the data included are:

Accepted FRP Cost (LS-$) = 7,202 + 68.53*FRP Area(ft^2)   (13)

Accepted FRP Cost (Q (M)-$) = 6,036 + 63.10*FRP Area(ft^2)   (14)

The coefficient of determination values obtained are 0.898 (LS, R^2) and 0.806 (Q (M), R*) respectively.

Scatter plot (Figure 3.3) is plotted between the accepted FRP cost and FRP area for all the bridges in California.

Bridges with accepted FRP cost of less than 1% of the total contract cost are omitted in this paper. Contract No. 08-472304 (Table 3.5) was found to have value of 0.10% and was not considered in the study to be consistent with the Oregon study, but it did not appear to be an outlier in the California data. Contract No. 08-0G4804 is a seismic retrofit, which had a different repair procedure than the rest of the bridges and much higher unit costs. Hence it was not considered in the analysis. The regression equations are computed again whithout these two bridges.
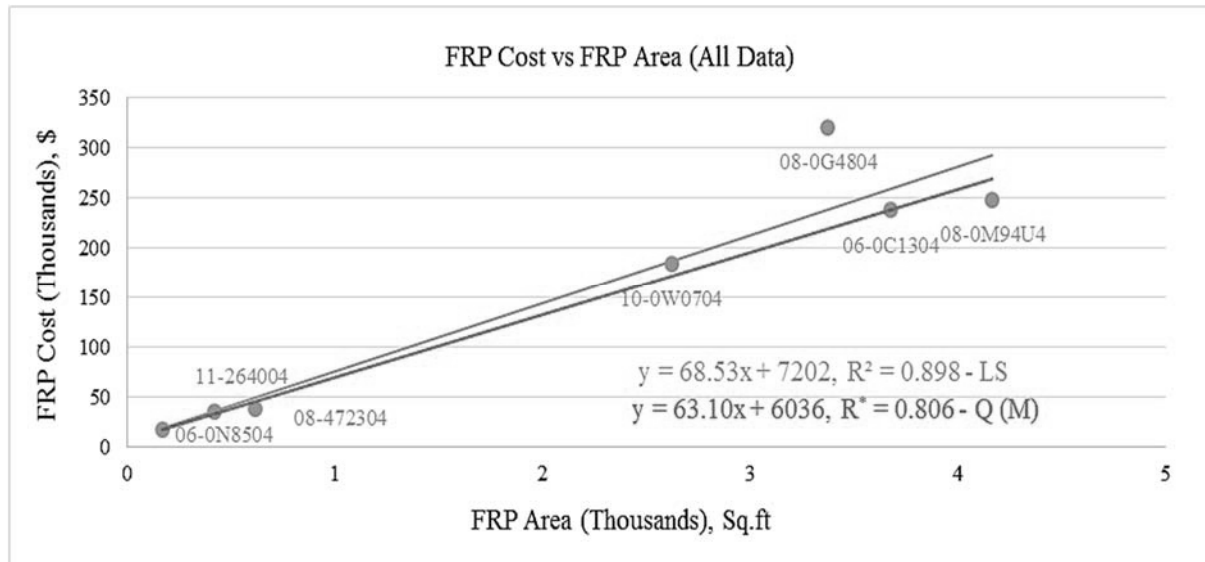
Figure. 3.3: Scatter Plot (All Data) of Accepted FRP Cost and FRP Area of California Highway Bridges (LS, Q (M)) with $R^2 = 0.898$ & $R^* = 0.806$

The regression equation obtained for accepted FRP cost against the FRP area for the bridges in California by LS regression method with an R^2 value of 0.991 is given by:

Accepted FRP Cost (LS-$) = 11,609 + 60.12*FRP Area(ft^2)   (15)

The regression equation obtained by Quantile (M) regression method for California bridges with R^* value of 0.926 is given by:

Accepted FRP Cost (Q (M)-$) = 9,322 + 62.20*FRP Area(ft^2)   (16)

Figure 3.4 shows the scatter plot of accepted FRP cost against FRP area of California bridges by the two analysis methods (LS, Q (M)) without the bridges - 08-

472304 & 08-0G4804. The high slope value of 62.20 for Quantile (M) and 60.12 for Least Square is due to higher FRP cost associated with the repairs. The slope difference (absolute) between the CERs of Figure 3.3 and Figure 3.4 is 0.90 (Q (M)) and 8.41 (LS) which indicates the robustness of Q (M) regression with respect to outliers.

The results from Table 3.6 show that Least Square regression method has the least SSE value and Quantile (M) regression method has the least MAD and MAPE values. The Quantile (M) regression method reduced the MAPE value from 10.01 to 4.25 than that of Least Square regression method. The major difference between the two methods is the better prediction of the Quantile method for the smallest area.
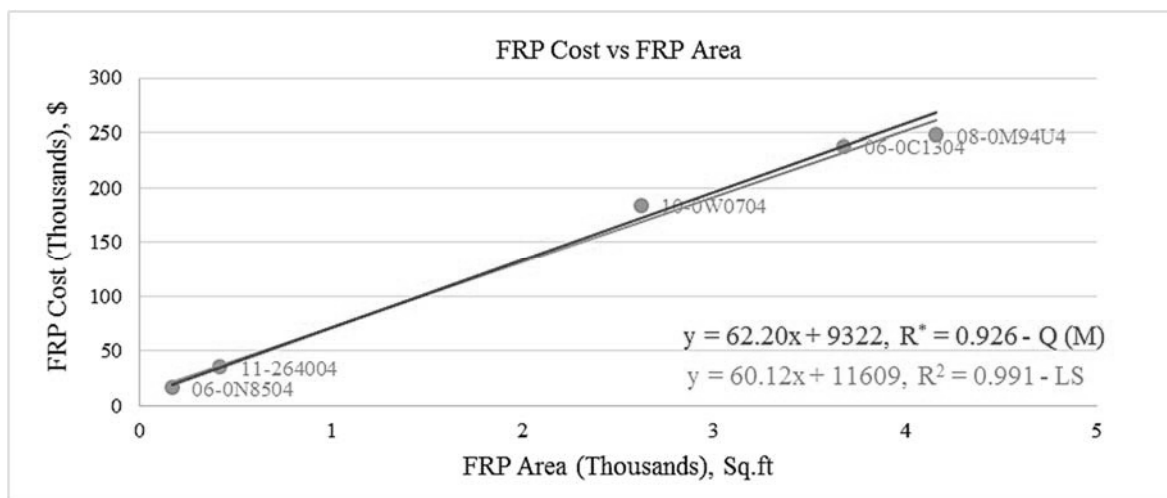
Figure 3.4: Scatter Plot of Accepted FRP Cost and FRP Area of California Highway Bridges (LS, Q (M)) with $R^2 = 0.991$ & $R^* = 0.926$

Table 3.6: Residual Analysis Table for California Highway Bridges

Area, ft²	Accepted FRP Cost, $	Predicted FRP Cost, $		SSE (X-Xp)^2	
		Least Square	Quantile (Median)	Least Square	Quantile (Median)
170	16,763	21,830	17,898	25,676,719	1,287,365
420	35,449	36,861	35,449	1,992,953	0
2,620	183,974	169,129	172,302	220,370,462	136,228,091
3,677	238,053	232,678	238,054	28,889,830	1
4,163	248,157	261,897	268,286	188,797,658	405,183,847
Total	722,396	722,396	731,989	465,727,621	542,699,304

Area, ft²	MAD			MAPE, %	
	Least Square	Quantile (Median)		Least Square	Quantile (Median)
170	5,067	1,135		30.23	6.77
420	1,412	0		3.98	0
2,620	14,845	11,672		8.07	6.34
3,677	5,375	1		2.26	0
4,163	13,740	20,129		5.54	8.11
Average	8,088	6,587	**Average**	10.01	4.25

A relationship between the accepted FRP cost and the FRP area to predict the unit cost ($/ft²) values, can be established. The predicted unit costs obtained from Equations 15 & 16 are given by:

Unit Cost (LS-$/ft²) = 60.12 + 11,609/FRP Area(ft²)

(17)

Unit Cost (Q (M)-$/ft²) = 62.20 + 9,322/FRP Area(ft²)

(18)

Table 3.7 shows the predicted FRP unit cost ($/ft²) values obtained by the two methods (LS & Q (M)) of

analysis for individual bridges. The actual FRP unit costs versus predicted FRP unit costs have good agreement overall, but the predicted equations are approximate only. There is the assumption that the start-up costs, which is indicated by the intercept of the curve, is constant for all project sizes. The fit is better for the California equations as the intercept values are small than those for the Oregon equations. When the bridges are grouped into two ranges as done in Table 3.8, the agreement is much better for the unit costs.

Table 3.7: Summary of FRP Repair Unit Cost ($/Ft^2) Obtained for Respective Areas of California Highway Bridges

Area, ft^2	Actual Cost, $	Actual FRP Unit Cost, $/ft^2	Pred. Unit Cost, $/ft^2 (LS)	Pred. Unit Cost, $/ft^2 (Q (M))
170	16,763	98.61	128.41	105.28
420	35,449	84.40	87.76	84.40
2,620	183,974	70.22	64.55	65.76
3,677	238,053	64.74	63.28	64.74
4,163	248,157	59.61	62.91	64.45

Table 3.8 shows for California bridges the FRP unit cost decreased as the area increased and the average FRP unit cost is approximately $64/ft^2 for areas greater than 2,000 ft^2.

Table 3.8: Summary Average FRP Unit Cost ($/ft^2) Obtained for Respective Area Range of California Bridges

FRP Area Range, ft^2	Average* FRP Unit Cost, $/ft^2 (LS)	Average* FRP Unit Cost, $/ft^2 (Q (M))	Average* FRP Unit Cost, $/ft^2 (Actual)
<2000	99.47	90.42	88.49
>2000	63.45	64.88	64.07

*The area of the respective bridges was considered as weight in calculating the average FRP unit cost

4 . Conclusions

There is a need for an effective cost estimation methodology in the transportation industry especially in the case of construction and rehabilitation of bridges. A brief introduction of Least Square regression and Quantile (M) regression was presented. The data of Oregon and California highway bridges was used to develop linear models for cost estimation of FRP wraps. The linear models obtained were used to compare the properties of the two methods based on graphical analysis and three test statistics (Mean Absolute Deviation (MAD), Mean Absolute Percentage Error (MAPE) & Sum of Square of Errors (SSE)). After the comparisons, the Quantile (M) regression had better properties in two aspects:

- Quantile (M) regression was found to have lower MAD and MAPE values, thus indicating the median improved the proximity of the CER to the data (Tables 3.2 & 3.6).
- Graphical analysis of results showed Quantile (M) regression to be robust to outliers. One or more outliers far away from the rest of the data had minimal impact on the predicted values. Quantile (M) regression did not favor high-cost values to the detriment of low-cost values as illustrated in Figures (3.1, 3.2, 3.3 & 3.4). The

slope difference (absolute) obtained between the CERs of Figures (3.1 & 3.2) of Oregon bridges is 0 (Quantile (M)) and 11.84 (Least Square) and for California bridges (i.e. between CERs of Figures (3.3 & 3.4)) is 8.41 (LS) and 0.90 (Q (M)) respectively. The low slope difference value for CERs of Quantile (M) regression validates the robustness of the method.

Based on the observations made in this study Quantile (Median) regression would be the preferred method of analysis when the data is large and scattered (Figure 3.1). When the mean and median are closer the differences become small between the two methods as indicated by Figure 3.4.

The analysis of the Oregon and California data was focused on developing relationships between FRP cost and FRP area by using Least Square and Quantile (M) analysis methods to predict the unit cost of FRP repair work. The high coefficient of determination values (0.884 (LS) & 0.773(Q) for Oregon, and 0.991(LS) & 0.926 (Q) for California) indicate FRP area to have a significant influence on the FRP cost. The FRP units cost curves are better predictors when the intercepts of

the linear FRP cost curves are small. The coefficient of determination values of Quantile (M) regression are lower than that of Least Square regression since the metric R^2 minimizes the sum of square of errors, which

is an inherent property of Least Square regression. The effect of outliers is much less with the Quantile (M) regrerssion than with the Least Square regression.

REFERENCES

[1]   3f. (2014, november 04). *3f-fr*. Retrieved November 13, 2014, From 3f-fr: http://3f-fr.com/?lang=en.

[2]   Barrodale, I. and Roberts, F. D. K., "Solution of an overdetermined system of equations in the L1 norm." *Communications of the Association for Computing Machinery*, 17, pp 319 320. 1974

[3]   Buhai, S. "Quantile regression: Overview and selected applications," *Ad-Astra-The Young Romanian Scientists' Journal, 4,* 2004

[4]   Foussier, P. "Improving CER Building:Basing A CER On The Median". *Journal Of Cost Analysis And Parametrics*, 1-3.24, 2010

[5]   Hald, A. "A History Of Parametric Statistical Inference From Bernoulli To Fisher,1713-1935," *Choice Reviews Online* , 44-6209-44-6209.25., 2007

[6]   Koenker, R. . *Quantile Regression*. Cambridge: Cambridge University Press, 1-30, 2005

[7]   Koenker, R. W., & d'Orey, V. "Algorithm AS 229: Computing regression quantiles," *Applied Statistics*, 383-393, 1987

[8]   ORDINARY   LEAST   SQUARES REGRESSION (Social Science). (n.d.). Retrieved June 30, 2014, From http://what-when-how.com/social-sciences/ordinary-least-squares-regression-social-science/.

[9]   Ordinary Least Squares Regression. (2008). In W. A. Darity, Jr. (Ed.), *International Encyclopedia of the Social Sciences* (2nd ed., Vol. 6, pp. 57-61). Detroit: Macmillan Reference USA.

[10]   Xia, S. *The Multicollinearity Problem-A Comparison Of Ordinary Least Squares And Some Alternative Regression Methods*. Ann Arbor: Copyright Proquest, UMI Dissertations Publishing 2009.

Appendix 1: Identifying The Outliers in Oregon Highway Bridges Data

Year	Bridge No.	FRP Area, ft²	Accepted Total FRP Cost, $	Predicted FRP Cost (ALL Points), $	Deviation 1	Deviation 2	Relative Variation %	R² (With Data Point Eliminated) 0.278
2007	01786A	3,144	159,343	105,282	54,062	57,829	6.5	0.281
2008	07601B	712	29,062	68,332	-39,270	-43,855	-7.91	0.251
2008	08381S	1,280	50,299	76,962	-26,662	-29,094	-4.19	0.265
2008	7458*	1,955	190,020	87,217	102,803	137,545	-59.93	0.352
2008	08383N	6,103	167,665	150,238	17,427	21,641	7.27	0.23
2009	8843*	2,345	250,480	93,142	157,337	168,017	18.42	0.449
2009	03173A*	9,204	124,069	197,351	-73,282	-159,297	-148.37	0.429
2010	7530	500	30,557	65,111	-34,555	-39,010	-7.69	0.248
2010	7532	500	30,557	65,111	-34,555	-39,010	-7.69	0.248
2010	7534	500	30,557	65,111	-34,555	-39,010	-7.69	0.248
2010	06945A	840	32,739	70,277	-37,538	-41,671	-7.13	0.254
2010	04981A	1,900	60,022	86,381	-26,360	-28,310	-3.36	0.273
2010	02233A	1,900	76,391	86,381	-9,990	-10,730	-1.27	0.275
2010	04979A	2,600	72,026	97,017	-24,991	-26,659	-2.88	0.28
2010	02236A	3,200	87,304	106,132	-18,828	-20,156	-2.29	0.282
2010	7392	5,800	174,609	145,634	28,975	35,016	10.43	0.227

*Outliers

Discharge Coefficient of Sharp-Crested Trapezoidal Labyrinth Weirs

Omer BILHAN[1]
M. Emin EMIROGLU[2]

Abstract

Labyrinth weirs provide an effective means to increase the spillway discharge capacity of dams and are often considered for renovation projects required due to an increase in expected flood inflow to the reservoir of an existing dam. Free crest spillways are hydraulically efficient and safe in operation. Since their discharge capacity is directly proportional to the crest length several types have been developed with the purpose to increase the length of the latter. In recent years many research investigations have considered the hydraulic performance of labyrinth weirs, particularly as dependent on the geometric features. The previous work has improved the design basis for such weirs. In the present study, discharge coefficients were experimentally determined for sharp crested trapezoidal labyrinth weirs of varying side wall angle (α). The experimental results of 21 physical models were used to develop a hydraulic design and analysis method for labyrinth weirs. The present research primarily aims at evaluating various characteristics of a flow-over labyrinth weir by conducting experimentations at wider range of values for important parameters.

Keywords*: Fluid mechanics, weir, discharge coefficient, trapezoidal, labyrinth weir*

1. Introduction

Spillways play a major role in ensuring the flood safety of dams. Insufficient spillway capacity has been the cause of one-third of all dam failures. Labyrinth weirs provide higher discharge capacity than conventional weirs, with the ability to pass large flows at comparatively low heads. A labyrinth weir is a linear weir that is 'folded' in plan-view to increase the crest length for a given channel or spillway width. Due to the complex design of the overflow structure, the labyrinth spillway discharge capacity is affected by many factors including weir geometry and approach channel conditions [1]. There is great flexibility in the geometric design of labyrinth

weirs. Yet, optimizing the many geometric variables in the hydraulic design of a labyrinth weir can be challenging. For example, the sidewall angle (*α*), total crest length (*L$_c$*), crest shape, number of cycles (*N*), the configuration of the labyrinth cycles, and the orientation and placement of a labyrinth weir must all be determined. A labyrinth weir is a linear weir that is 'folded' in plan-view to increase the crest length for a given channel or spillway width [2]. Figure 2 provides the key details of the labyrinth weir. The distinguishing characteristic of labyrinth spillways is that the plan shape is not linear but varies using a repeating planform as U shape (eventually rectangular), V or triangular shape (Figure 1 (a)) and trapezoidal shape (Figure 1 (b)).

---

[1] *Nevsehir H.B.V. University, Nevsehir, Turkey, obilhan@nevsehir.edu.tr*

[2] *Firat University, Elazig, Turkey*

(a)   **(b)**
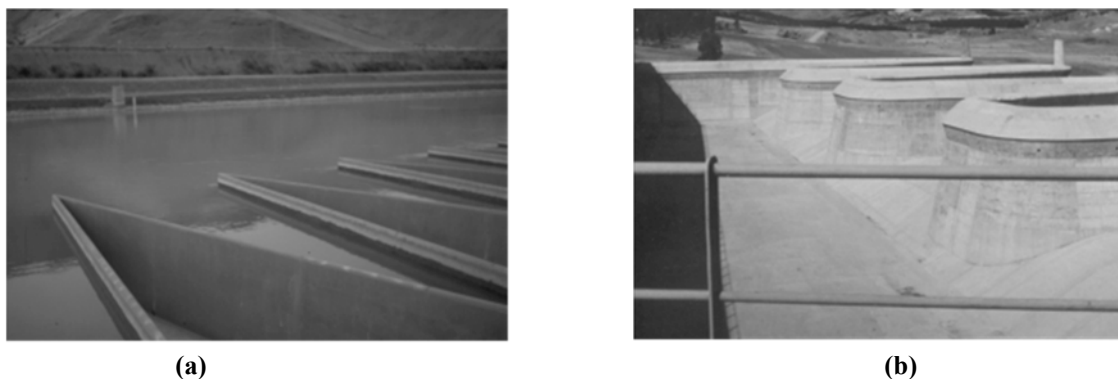
Figure 1. **(a)** Triangular labyrinth weir of the hydroelectric power plant Ohau C in New Zeland. **(b)** Trapezoidal labyrinth weir of Cimia dam in Italy.

Optimizing the many geometric variables in the hydraulic design of a labyrinth weir can be challenging. For example, the sidewall angle (α), total crest length (L_c), crest shape, number of cycles (N), the configuration of the labyrinth cycles, and the orientation and placement of a labyrinth weir must all be determined. Furthermore, the geometry of a labyrinth weir causes complex 3-dimensional flow patterns that must be considered. The flow rate passing over the labyrinth is dependent on the crest length, which can be controlled by modifying the number of folds. The relationship between length and discharge is not linear, however, except for very small heads. As the water level above the labyrinth weir increases, four stages of nappe shape occur: fully aerated, partially aerated, transition and submerged. The thickness of nappe and depth of the tailwater do not affect the discharge capacity of the labyrinth weir in the fully aerated flow condition. In this case, the labyrinth weir acts as a vertical cross section of the linear weir. As the water level above the labyrinth weir increases and the tailwater rises, the nappe becomes partially aerated (adhering to the weir wall) and the discharge coefficient is reduced [3-4].

In recent years, extensive research on the influence of geometric and hydraulic parameters on the hydraulic behavior of labyrinth weirs, particularly on the discharge capacity, has been completed. Taylor (1968) [5] presented initial studies on the behavior of labyrinth weirs and presented the hydraulic performance as it compares with that of sharp-crested weirs. Hay and Taylor [6] followed up on Taylor's

work and developed design criteria for labyrinth weirs. Based on their research findings, they suggested Eq. (1) for the discharge coefficient of labyrinth weirs.

$$C_d = 3.22 + 0.40 \frac{h}{P} \qquad (1)$$

where C_d is the discharge coefficient, h is the depth of flow over the weir crest and P is the weir height.

Additional work by Darvas [7] utilized the results from physical model studies to expand on the theory and develop a family of curves to evaluate spillway performance. Extensive physical model studies were performed by Houston [8] to evaluate various labyrinth geometries and approach conditions. The U.S. Bureau of Reclamation (USBR) tested a model of labyrinth spillway for Ute Dam and Hyrum Dam [8-9]. They found that the discrepancy between their observations and those of Hay and Taylor (1970) [6] were caused by difference in head definition. has also investigated model studies of the labyrinth weir and Eq. (2) is his suggested equation for calculation of discharge over labyrinth weirs.

$$Q = C_d \left(\frac{\dfrac{Wc}{P}}{\dfrac{Wc}{P+K}} \right) W_c H_t \sqrt{gH_t} \qquad (2)$$

where Q is the discharge over labyrinth weir, C_d is the discharge coefficient, H_t is the total upstream head

measured relative to the weir crest, W_c is the channel width and P is the weir height.

Magalhaes and Lorena [11] calculated discharge coefficient (C_d) of labyrinth weirs as function of L/w and H_t/P parameters. They defined discharge capacity of labyrinth weirs with Eq. (3).

$$Q = C_d W_T 2gH_t^{1.5}$$ (3)

Tullis et al. [12] carried out extensive experimental work on the performance of the labyrinth weir. They proposed a flow equation for the labyrinth weir that is identical to the basic equation applicable to a linear weir, but with modification of the coefficient of discharge. They also presented experimental data of the variation of discharge coefficient of labyrinth weir with a head to weir height ratio (H_t/P) for side wall angles (α) of 6° to 18°. Additional curves for weir side angles of 25° and 35° were obtained by extrapolation. Tullis et al. (2007) [13] extended this work by providing a dimensionless head-discharge relationship for submerged labyrinth weirs. Using a physical model of the labyrinth weir of Dog River Dam in Georgia, Savage et al. [14] showed that the method of Tullis et al. [12] produced a discharge error up to ± 25% .

Labyrinth weirs are also used as side weirs to increase the outflowing discharge. Emiroglu et al. [15] carried out extensive experimental work on the performance of the labyrinth side weirs and presented coefficient of discharge curves in a simplified way as compared to previous investigators. Further work on triangular labyrinth side weirs was completed by Bilhan et al. [16] using Artificial Neural Network (ANN) techniques to calculate the discharge coefficient under critical flow conditions.

Khode et al. [17] carried out flume studies on trapezoidal labyrinth weirs for side wall angles 6°, 8°, 10°, 16°, 21°, 26° and 30°. Khode et al. [18] extended these studies for a wider range of flow conditions.

Anderson and Tullis [19] used laboratory-scale physical models to compare the hydraulic efficiency

of the Piano Key (PK) weir design with that of a geometrically similar rectangular labyrinth weir, with and without sloping floors installed in the inlet and outlet keys. The test data showed that the PK weir was more efficient than the geometrically comparable rectangular labyrinth weir, a fact likely attributable to a reduction in entrance losses associated with the PK weir inlet key geometry.

Crookston and Tullis [20] published labyrinth weir design equations that are applicable to in-channel labyrinth weir applications in which the approach flow is oriented normal to the weir axis. Consequently, some uncertainty exists regarding the hydraulic performance of labyrinth weir configurations that deviate from the experimental conditions associated with the empirical determinations.

Anderson and Tullis [19] investigated 9 laboratory-scale four-cycle PK weir configurations to develop a better understanding of the effects of PK weir geometry on discharge efficiency. The appropriateness of the recommended head-discharge equation specific to the recommended design was evaluated, and the relative head-discharge efficiency of trapezoidal labyrinth and PK weirs with respect to footprint restrictions and crest length were compared in this study.

Information regarding nappe aeration conditions (clinging, aerated, partially aerated, and drowned), nappe instability, and nappe vibrations for trapezoidal labyrinth weirs on a horizontal apron with quarter- and half-round crests (6° $\leq \alpha \leq$ 35°) was presented by Crookston and Tullis [21]. In this study, hydraulic behaviors associated with nappe aeration conditions were recommended to aid in labyrinth weir design, related to nappe behavior (e.g., crest shape, crest roughness, vents, nappe breakers, notches, and staged cycles) in future studies.

While all these documented studies have provided significant insights to the behavior of labyrinth weirs under specific conditions, the general theory remains: the capacity of labyrinth weir is a function of the upstream total head, the effective crest length, and the coefficient of discharge. The discharge coefficient

depends on the total head, weir height, thickness, crest shape, apex configuration, and angle of side wall. While viscosity and surface tension are also significant variables, their influence is limited at velocities of sufficient magnitude and by appropriate model geometries [19]. The purpose of this study is to systematically investigate the discharge capacity of sharp-crested trapezoidal labyrinth weir using a broad range of experiments, and considered together with the

other effective dimensionless parameters. Most of the design and performance information regarding labyrinth weirs has been developed from physical model studies, often for a specific prototype installation (e.g., Avon, Dungo, Hyrum, Keddara, Lake Brazos, Lake Townsend, Ute, and Woronora). A selection of notable research studies that have provided hydraulic design guidance for labyrinth weirs is presented in Table 1.

Table 1. Labyrinth Weir Design Methods

|	Authors	Labyrinth Cycle Type	Crest Shape
1	Taylor (1968), Hay and Taylor (1970) [5-6]	Tri, Trap, Rect	Sh, HR
2	Darvas (1971) [7]	Trap	LQR
3	Hinchliff and Houston (1984) [23]	Tri, Trap	Sh, QR
4	Lux and Hinchliff (1985) [24]	Tri, Trap	QR
5	Magalhães and Lorena (1989) [11]	Trap	WES
6	Tullis et al. (1995) [12]	Trap	QR
7	Melo et al. (2002) [25]	Trap	LQR
8	Tullis et al. (2007) [13]	Trap	HR
9	Lopez et al. (2008) [26]	Trap	LQR

Tri = Triangular, Trap = Trapezoidal, Rect = Rectangular, QR –Quarter-round (Rcrest = tw/2), LQR – Large Quarter-round (Rcrest = tw), HR – Half-round, Sh – Sharp, WES – Truncated Ogee

2. Experimental Method

21 physical models of labyrinth weirs were fabricated and tested at the Firat University Hydraulic Research Laboratory, located in Elazig, Turkey [22]. The experimental set-up includes sump, pumping system, discharge tank, rectangular flume, digital flowmeter and labyrinth weir. Water is recirculated through 250 mm diameter of supply line using two 75 HP pumps. Water for experimental setup is taken from the supply line by means of a pipe with 150 mm diameter. The discharge was measured by means of a Siemens electromagnetic flow-meter installed in the supply line. Water was supplied to the main channel (2 m wide and 0.80 m

height this channel length is 3.0 m) through a supply pipe from the sump (volume of 15 m^3) with flow controlled by a gate valve. For damping the water surface waves and reducing turbulence, baffle wall and wood surface dampener is provided. In the experiments, the upstream elevation was built higher than the downstream elevation so that free flow conditions occur downstream of the weir. Sheet metal materials which have 4 mm thickness (*t*) were used for labyrinth weirs. Labyrinth weirs designed as three-cycles. Schematic view of trapezoidal labyrinth weirs is given in Fig. (2). Each trapezoidal labyrinth weir models with a sharp crested shape was tested in the experiments (Examples shown in Fig. (3)).
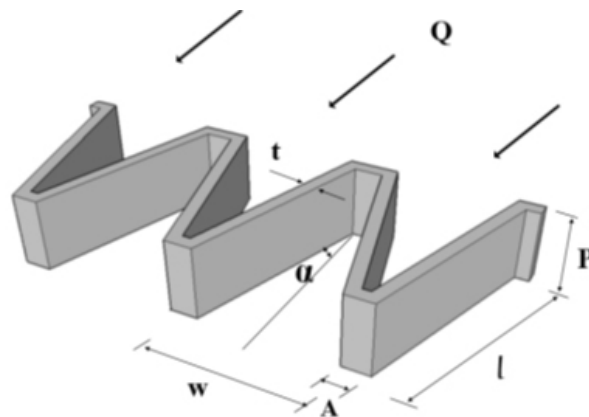
Figure 2. Schematic view of the trapezoidal weirs located on straight channel

Figure 3. Experimental set-up for Trapezoidal labyrinth weirs

To measure the nappe height, water depth was measured accurately using Mitutoyo digital point gauges (accurate to ±0.01 mm) just upstream of the weirs. Level measurements were taken at a distance from the weir equal to five times the nappe height. For flow rate measurements, Nortek brand acoustic three-axis velocimeter was used.

In the experiments, the weir heights were taken as 100 mm, 150 mm and 200 mm and apex width (*A*) was taken as 80 mm. Sharp-crested shapes is provided for all models. All experiments were performed according to free flow conditions.

The flow over labyrinth weir is three dimensional and does not readily fit into mathematical description and hence the discharge function is found through experimental studies and analysis. The crest coefficient depends on the total head, weir height, thickness, crest shape, apex configuration and angle of side wall. To simplify the analysis, the effect of viscosity and surface tension could be neglected by selecting model and velocity of sufficient magnitude. The discharge over labyrinth weir can be expressed as:

$$Q = \frac{2}{3} C_d \sqrt{2g} H_t^{1.5} L \qquad (4)$$

Where Q is the discharge over a labyrinth weir; C_d is the discharge coefficient of the labyrinth weir; L is the effective length of labyrinth weir; H_t is the total head $(V_0^2/2g + h)$ and g is the gravitational acceleration constant (Fig 4).
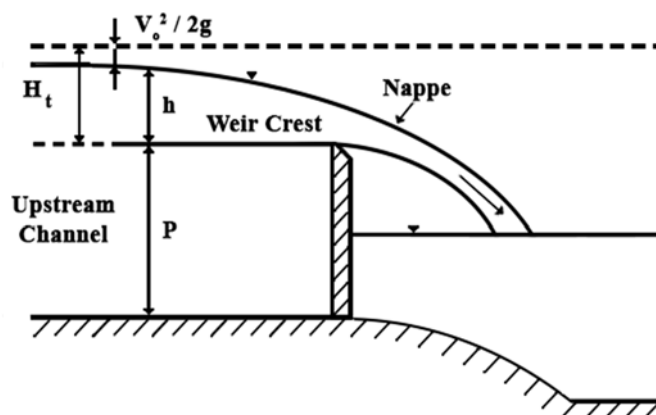
Figure 4. Definition sketch for flow over a sharp crested weir

Head over labyrinth weir was measured for different value of discharges in the range of 14.7 L⁄s to 136.9 L⁄s. In this range, the head over the labyrinth weir varied from 10 to 90 mm. The model of linear weir is also tested in the same flume for the purpose of comparison.

In an effort to develop a better understanding of the hydraulic characteristics of trapezoidal labyrinth weirs, with this experimental research was undertaken. Table 2 gives the description of different types of the trapezoidal labyrinth weirs tested.

Table 2. Physical model test program in the present study

Model	W_c (cm)	P (cm)	L (cm)	N	A (cm)	L_c/w	Type of Weir
1	196	10	196	-	-	-	Linear Weir, α=90°
2	196	10	294	3	8	1.50	Trapezoidal Labyrinth Weir, α=37°
3	196	10	345	3	8	1.76	Trapezoidal Labyrinth Weir, α=30°
4	196	10	427	3	8	2.18	Trapezoidal Labyrinth Weir, α=23°
5	196	10	534	3	8	2.73	Trapezoidal Labyrinth Weir, α=18°
6	196	10	621	3	8	3.17	Trapezoidal Labyrinth Weir, α=15°
7	196	10	774	3	8	3.95	Trapezoidal Labyrinth Weir, α=12°
8	196	15	196	-	-	-	Linear Weir, α=90°
9	196	15	294	3	8	1.50	Trapezoidal Labyrinth Weir, α=37°
10	196	15	345	3	8	1.76	Trapezoidal Labyrinth Weir, α=30°
11	196	15	427	3	8	2.18	Trapezoidal Labyrinth Weir, α=23°
12	196	15	534	3	8	2.73	Trapezoidal Labyrinth Weir, α=18°
13	196	15	621	3	8	3.17	Trapezoidal Labyrinth Weir, α=15°
14	196	15	774	3	8	3.95	Trapezoidal Labyrinth Weir, α=12°
15	196	20	196	-	-	-	Linear Weir, α=90°
16	196	20	294	3	8	1.50	Trapezoidal Labyrinth Weir, α=37°
17	196	20	345	3	8	1.76	Trapezoidal Labyrinth Weir, α=30°
18	196	20	427	3	8	2.18	Trapezoidal Labyrinth Weir, α=23°
19	196	20	534	3	8	2.73	Trapezoidal Labyrinth Weir, α=18°
20	196	20	621	3	8	3.17	Trapezoidal Labyrinth Weir, α=15°
21	196	20	774	3	8	3.95	Trapezoidal Labyrinth Weir, α=12°

3. Experimental Results

Experiments are carried out on six trapezoidal labyrinth weir models having side wall angles of 12°, 15°, 18°, 23°, 30° and 37° and a linear weir models having sharp crested shape similar to labyrinth weirs models. On all these models, head-discharge measurements are taken for weir height of P=10, 15 and 20 cm.

Discharge coefficient for trapezoidal labyrinth weirs was computed using equation (Eq. (4)). Discharge coefficients of trapezoidal labyrinth side weirs have much higher values than the conventional weirs. The effect of crest shape on the discharge coefficient is very significant for the same channel width and crest length.

From these experiments, the variation of C_d for trapezoidal labyrinth weirs with H_t/P is plotted for P=10, 15 and 20 cm in Fig.5. It is noted that discharge coefficient for labyrinth weirs is computed using equation (Eq. (4)). It is apparent from the results in Fig. 5 that discharge capacity of the labyrinth weirs is much higher than the conventional weirs. The primary reason for this is that the crest length of the labyrinth weir is much longer than that of the conventional weir. Similarly, to establish a relationship between L_c/w with C_d the observed data are plotted and shown in Fig.6. The layouts of labyrinth weir should be normally designed for maximum value of C_d max and the design curve developed from this present experimental study would help the designer to design trapezoidal labyrinth weir. The coefficient of discharge C_d is minimum for side wall angle of 12 degree and increases with increase in side wall angle approaching the value of linear weir.
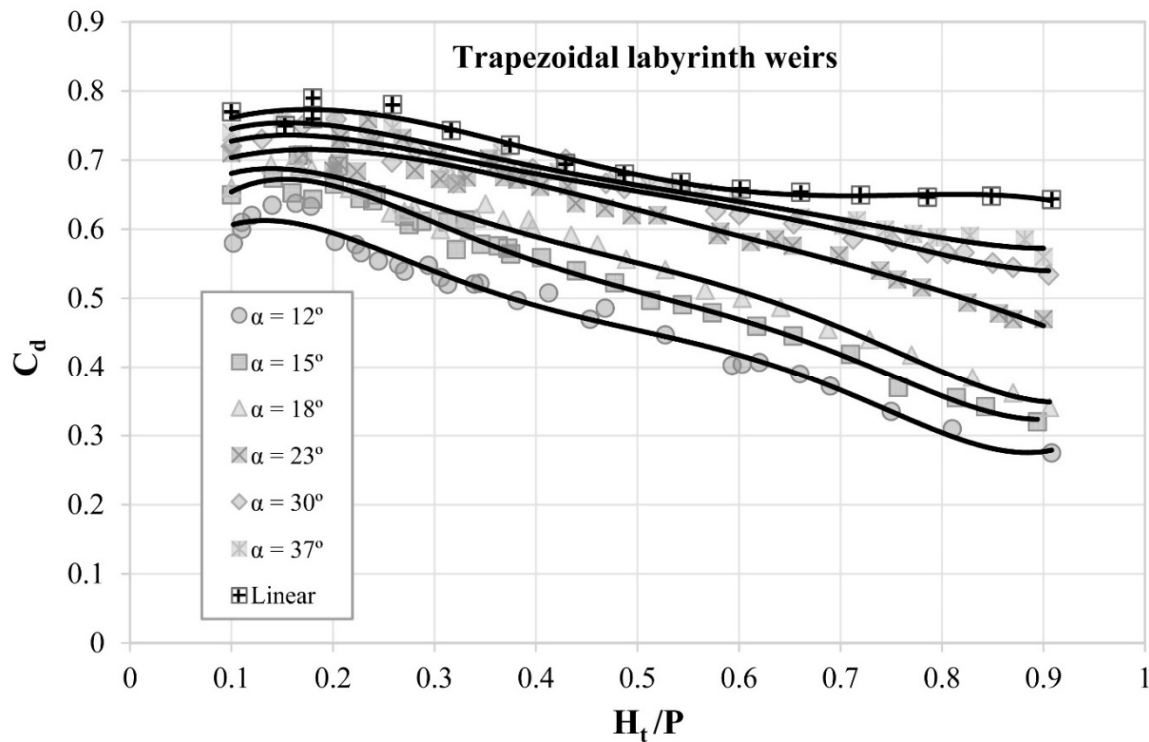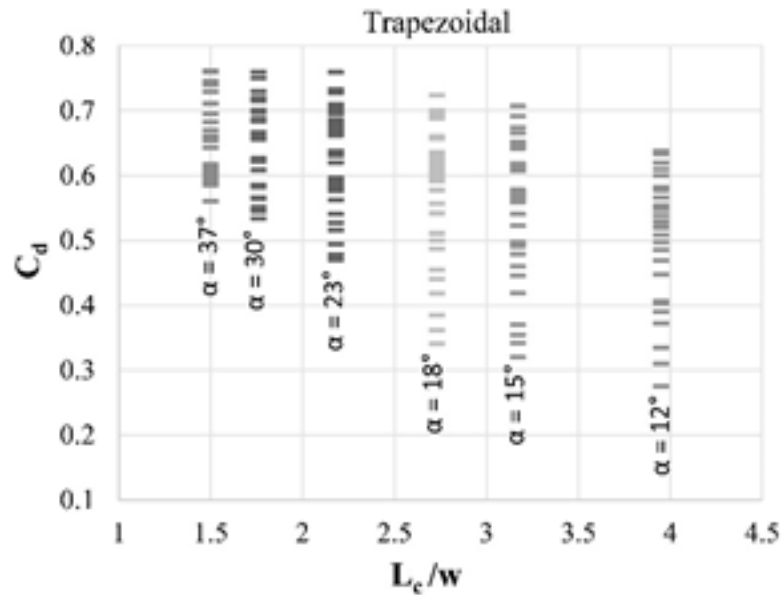

Figure 5. Variation of discharge coefficient (C_d) with head to weir height (H_t/P) for trapezoidal labyrinth weirs

Figure 6. Variation of discharge coefficient (C_d) with L_c/w for trapezoidal labyrinth weirs

To represent the data of the equation form, correlation analysis is carried out for the observed data for each model, separately. The 5th degree polynomial provides a reasonable fit between C_d and H_t/P. Thus, discharge coefficient (C_d) of sharp-crested labyrinth weir is expressed as:

$$C_d = A_0 + A_1\left(\frac{H_t}{P}\right) + A_2\left(\frac{H_t}{P}\right)^2 + A_3\left(\frac{H_t}{P}\right)^3 + A_4\left(\frac{H_t}{P}\right)^4 + A_5\left(\frac{H_t}{P}\right)^5 \tag{5}$$

The values of C_d, A_0 to A_5 and R^2 are shown in Table 3.

Table 3. Coefficient of discharge per unit length of trapezoidal labyrinth weir

Model	A_0	A_1	A_2	A_3	A_4	A_5	R^2
Trapezoidal, α =12°	0.4598	2.8255	- 17.296	40.718	- 43.59	17.273	0.9799
Trapezoidal, α =15°	0.4600	3.4773	- 19.171	42.242	- 43.039	16.438	0.9848
Trapezoidal, α =18°	0.5638	2.1933	- 12.876	29.283	- 30.857	12.090	0.9738
Trapezoidal, α =23°	0.6417	0.9673	- 4.0152	5.7463	- 3.8338	0.8922	0.9608
Trapezoidal, α =30°	0.6395	1.5467	- 8.3233	17.937	- 18.184	6.9522	0.9620
Trapezoidal, α =37°	0.6537	1.6113	- 8.6152	18.076	- 17.719	6.5955	0.9790
Linear	0.6991	0.9370	- 3.4166	2.4939	1.8340	-1.9528	0.9665

The discharge coefficient values of labyrinth weir compared well with those of Woronora Dam, Boardman Dam, and Avon Dam. Moreover, the results of the present study compared well with those of Tullis et al. [12], as shown in Fig.7. Although the data values are different, due to the variation in nappe shape and side wall angle for each study, the trends are similar to the findings of Tullis et al. [12] and prototype data.
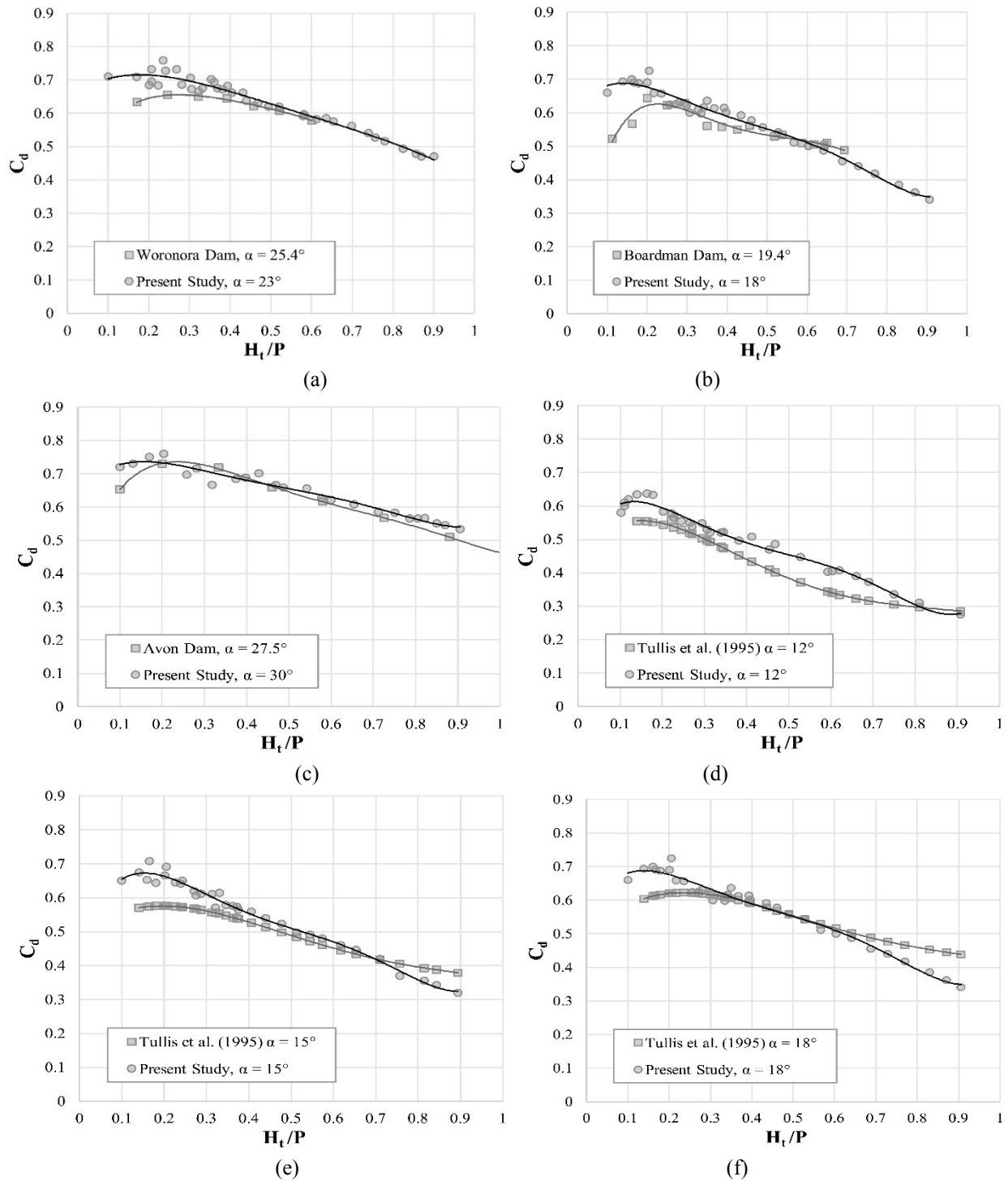
Figure 7. Variation of discharge coefficient (C_d) with head to weir height (H_t/P) for present study compared to other findings: (a) Woronora Dam [7], (b) Bordman Dam [27], (c) Avon Dam [7]; (d –f) data from Tullis et al. [12]

4. Conclusions

Labyrinth weirs can pass large flows at comparatively low heads. The crest shape is one of the most important factor which affects the discharge capacity for labyrinth weirs. According to this experimental study, it was found that the trapezoidal labyrinth weirs are hydraulically more efficient than the linear weirs from the perspective of ease of construction and the discharge capacity. The values for coefficient of discharge can be suitably obtained from the design curves and the regression equation generated through this study for trapezoidal labyrinth weirs. The values for discharge coefficient of trapezoidal labyrinth weirs can be suitably obtained from the design curves and the regression equations generated through this study for α between 12 to 37°. The coefficient of discharge C_d is minimum for side wall angle of 12 degree and increases with increase in side wall angle approaching the value of linear weir. Of course, given unlimited width, greater efficiencies (discharge per head) will be obtained for a linear weir. However, the trapezoidal provides much greater weir length in confined space with only limited reductions in efficiency (reduction in C_d).

A problem for labyrinth weirs is matching the outflow to downstream flow limitations. An example would be where previous water rights limit releases from the reservoir at floods below the hundred-year flood. If the labyrinth is to be added to an existing reservoir where the downstream requirements limit the flows at low water-surface elevations, a labyrinth with a small angle may provide more capacity than can be tolerated. For such an installation, a large angle labyrinth may better fit the outflow requirements. If the low flow requirement is extremely small, a short section of weir at a lower elevation could be used to pass small flows. The full labyrinth would not activate until the flood exceeds some predetermined level, such as the hundred-year flood. It is recommended that a labyrinth weir design be verified with a physical or numerical model study, as it would include site-specific conditions that may be outside the scope of this study and may provide valuable insights into the performance and operation of the labyrinth weir.

NOMENCLATURE

A	Apex width;
C_d	Discharge coefficient;
g	Acceleration constant of gravity;
h	Depth of flow over the weir crest;
H_t	Total upstream head measured relative to the weir crest;
H_t/P	Headwater ratio;
ℓ	Centerline length of weir sidewall;
N	Number of labyrinth weir cycles;
P	Weir height;
Q	Discharge over weir;
V	Average cross-sectional flow velocity upstream of weir;
W_c	Channel width;
w	Width of a single labyrinth weir cycle;
L	Total crest length of labyrinth weir;
L_c	Total crest length for a single labyrinth weir cycle;
R^2	Determination coefficient
t	Weir wall thickness

REFERENCES

[1] Yıldız D., Uzucek E. (1993) Labirent dolusavakların projelendirilme kriterleri. Devlet Su İşleri Teknik Araştırma Kalite ve Kontrol Dairesi Başkanlığı. Yayın No: HI-862 Ankara.

[2] Crookston, B. M., and Tullis, B. P. (2012b) Labyrinth weirs: Nappe interference and local submergence. J. Irrig. Drain. Eng., 138(8), 757–765.

[3] Yıldız, D., Uzucek, E. (1996) Modeling the performance of labyrinth spillways. Int. J. Hydropower Dams, 3, 71–76.

[4] Tsang, C. (1987) Hydraulic and aeration performance of labyrinth weirs. Ph.D. dissertation, University of London, London.

[5] Taylor, G. (1968). The performance of labyrinth weirs. PhD thesis, University of Nottingham, U.K.

[6] Hay, N., and Taylor, G. (1970) Performance and design of labyrinth weir. J. Hydraul. Eng., 96(11), 2337–2357.

[7] Darvas, L. (1971) Discussion of performance and design of labyrinth weirs, by Hay and Taylor. J. Hydraul. Eng., ASCE, 97(80), 1246–1251.

[8] Houston, K. (1982) Hydraulic model study of Ute dam labyrinth spillway. Rep. No. GR-82-7, U.S. Bureau of Reclamation, Denver.

[9] Houston, K. (1983) Hydraulic model study of Hyrum dam auxiliary labyrinth spillway. Rep. No. GR-82-13, U.S. Bureau of Reclamation, Denver.

[10] Lux, F., (1989) Design and Application of Labyrinth Weirs, Design of Hydraulic Structures 89, Balkema, Rotterdam, ISBN, 90, 6191 – 8987.

[11] Magalhaes, A., and Lorena, M. (1989) Hydraulic design of labyrinth weirs. Rep. No. 736, National Laboratory of Civil Engineering, Lisbon, Portugal.

[12] Tullis, B. P., Amanian, N., and Waldron, D. (1995) Design of labyrinth weir spillways. J. Hydraul. Eng., ASCE, 121(3), 247–255.

[13] Tullis, B. P., Young, J., and Chandler, M. (2007) Head-discharge relationships for submerged labyrinth weirs. J. of Hydraul. Eng., ASCE, 133(3), 248–254.

[14] Savage, B., Frizell, K., and Crowder, J. (2004) Brains versus brawn: The changing world of hydraulic model studies. ASDSO 2004 Annual Conf. Proc., Association of State Dam Safety Officials (ASDSO), Lexington, KY. (May 4, 2009).

[15] Emiroglu, M. E., Kaya, N., and Agaccioglu, H. (2010)."Discharge capacity of labyrinth side weir located on a straight channel."J. Irrig. Drain. Eng., ASCE, 136(1), 37–46.

[16] Bilhan, O, Emiroglu, M. E., Kisi, O, (2010) Use of artificial neural networks for prediction of discharge coefficient of triangular labyrinth side weir in curved channels. J. Advances in Eng. Soft. 42(4), 208-214.

[17] Khode, B.V., Tembhurkar, A.R. Porey, P.D. and Ingle R.N. (2011) Determination of Crest Coefficient for Flow over Trapezoidal Labyrinth Weir. World Applied Sciences Journal 12 (3): 324-329.

[18] Khode, B. V., Tembhurkar, A. R. P. D. Porey and R. N. Ingle, (2012) Experimental Studies on Flow over Labyrinth Weir. Journal of Irrig. Drain Eng. ASCE, 138:548-552.

[19] Anderson, R. M. and Tullis, B. P., (2012) Comparison of Piano Key and Rectangular Labyrinth Weir Hydraulics. J. Hydraul. Eng. 138:358-361.

[20] Crookston, B. M., and Tullis, B. P. (2012a) Arced labyrinth weirs. J. Hydraul. Eng., 138(6), 555–562.

[21] Crookston, B. M. and Tullis, B. P. (2013) Hydraulic Design and Analysis of Labyrinth Weirs. II: Nappe Aeration, Instability, and Vibration. J. Irrig. Drain Eng., ASCE, 139(5), 371–377.

[22] Emiroglu M. E., Omer Bilhan, "Investigation of discharge coefficient of labyrinth weirs and using nape breakers on this weirs." Project No: 1610, Firat University, FUBAP, 2009, Turkey.

[23] Hinchliff, D., and Houston, K. (1984). Hydraulic design and application of labyrinth spillways. Proc., 4th Annual USCOLD Lecture, Dam Safety and Rehabilitation, Bureau of Reclamation, U.S. Dept. of the Interior, Washington, DC.

[24] Lux and Hinchliff, (1985). "Discharge construction of labyrinth spillway." Transactions of 15th congress of international Committee on large Dam. Lausanne Switzerland, pp: 249-274.

[25] Melo, J., Ramos, C., and Magalhães, A. (2002) "Descarregadores com soleira em labirinto de um ciclo em canais convergentes. Determinação da capacidad de vazão". Proc. 6o Congresso da Água (CD-ROM), Associação Portuguesa dos Recursos Hídricos, Lisboa, Portugal.

[26] Lopez, R., Matos, J. and Melo, J. (2008) "Characteristic depths and energy dissipation downstream of a labyrinth weir." 2nd Int. Junior Researcher and Engineer Workshop on Hydraulic Structures, Pisa, Italia.

[27]   Babb, A. (1976). "Hydraulic model study of the Boardman Reservoir Spillway." R.L Albrook Hydraulic Laboratory, Washington State University, Pullman, Wash.

Performance Evaluation for MIPv6 IN Pure IPv6 Networks vs. 6 TO 4 IP Mechanism Networks using OPNET

Abdulkader OMAR ALWER[1]

Abstract

IPv6 protocol is the last protocol for IP protocol. IPv6 protocol based on 128 bits for addressing and has many features comparing with old one IP protocol (or which called IPv4 protocol) that is still using till now in many companies and based on 32 bits in addressing. Mobile IPv6 is protocol that using for mobile nodes that moves from it home place to other places and depends on IPv6.In our Study we will focus on implementing Mobile IPv6 MIPv6 in two networks, one is pure IPv6 network and another is mixed networks that consisting of IPv4 and IPv6 networks. We used in our study mechanism 6 to 4 to connect between IPv4 nodes and IPv6 nodes. In these two scenario Mobile node MN used MIPv6 between two access routers. The aim of this paper is to study IPv6 traffic inside MN and IPv4 and IPv6 internet clouds and finally throughput for WLAN using many kinds of application in this topology like FTP, Email, Terminal server applications. Optimized Engineering Tools (OPNET) 14.5 is used to verify of topology and get the results. The result of our study shows that working in pure IPv6 networks for MN and for Internet IPv6 clouds better than working in 6 to 4 networks. Although from these result, there is no different actually in IPv4 clouds when we using pure IPv6 and 6 to 4 IPv6 networks if we use it after IPv6 cloud.

Keywords: *IPv6, MIPv6, 6 to 4 IP mechanism, IPv4, OPNET*

1. Introduction

The Internet has been growing at a very fast rate during the last ten years. The Internet runs over IP version 4 (IPv4), but this protocol was designed 30 years ago for a few hundred computers. The number of globally unique unicast IPv4 addresses still available is not enough to assign a different IP address to every new device to come. IP is considered by the market as the common denominator to converge different application layers such as data, voice, and audio. However, these new devices require many more IP addresses to interconnect all kinds of IP appliances besides just the computers currently interconnected on the Internet. The size of an IPv6 address [1] is 128 bits, 4 times bigger than an IPv4 address; 32 bits' address space allows up to 4.294.967.296 combinations, while the 128 bits of an IPv6 address allows up to $3,4 \times 10^{38}$, therefore it is obvious the increase in available addresses.

In this paper, we focus on three important points: (1) Data traffics in Mobile node MN, (2) throughput in Wireless LAN and (3) traffics in IPv4 and IPv6 clouds

in pure IPv6 network and 6 to 4 IP network and analysis.

This paper is organized as follows: Section 1 is introduction, where is section 2 is related works, then section 3 theatrical information. Then section 4 provides practical study scenarios and compared results in our evaluation. Finally, section 5, present results and conclusion.

2. Related works

Many research and books study the connection between IPv4 and IPv6 [2],[3] that explained 6 to 4 method is very useful especially that does not needs to changes routers for IPv6 configurations. Comparison using OPNET between IPv6 and 6 to 4 networks studied has done in [4], but not for Mobile node (MN) it just for stationary and small company without take internet traffic in their considerations.[5]studies the scenarios to mobility between IPv4 and IPv6 networks without give any results or simulation on his works, we select in our

---

[1] *Assistant Professor in Istanbul Aydin University, Istanbul, Turkey, abdulalwer@aydin.edu.tr*

research mobility between two nodes inside IPv6 routers.

3. Theatrical Information
3.1. IPv6 Address
IPv4 addresses are represented in dotted-decimal format. The 32-bit IPv4 address is divided along 8-bit boundaries. Each set of 8 bits is converted to its decimal equivalent and separated by periods. For IPv6, the 128-bit address is divided along 16-bit boundaries, and each 16-bit block is converted to a 4-digit hexadecimal number and separated by colons. The resulting representation is called colon hexadecimal.

The network prefix in an IPv6 address is represented in the same way that IPv4, for example, take the IPv4 address 192.168.1.0/27, this means that the first 27 bits are network's and the remaining 5 are which identify a device, thus in IPv6 the following address ffe:b00:c18:1::1/64 indicates that the first 64 bits identifies the network (3ffe:b00:c18:1) and the remaining 64 bits identifies the device in that network (::1).
3.2. MIPv6

Mobile IPv6 [6], allows mobile node to move from one link to another without changing the mobile node's "home address". Packets may be routed to the mobile node using this address regardless of the mobile node's current point of attachment to the Internet. The mobile node may also continue to communicate with other nodes (stationary or mobile) after moving to new link. The movement of a mobile node away from its home link is thus transparent to transport and higher-layer protocols and applications.

3.2.1. Mobile IPv6 Operation
When a mobile node is away from home, it sends information about its current location to the home agent. A node that wants to communicate with a mobile node uses the home address of the mobile node to send packets. The home agent intercepts these packets, and using a table, tunnels the packets to the mobile node's care-of address.
Mobile IPv6 uses care-of address as source address in foreign links. Also, to support natural route optimization, the Correspondent node uses IPv6 routing header than the IP encapsulation fig. (1).
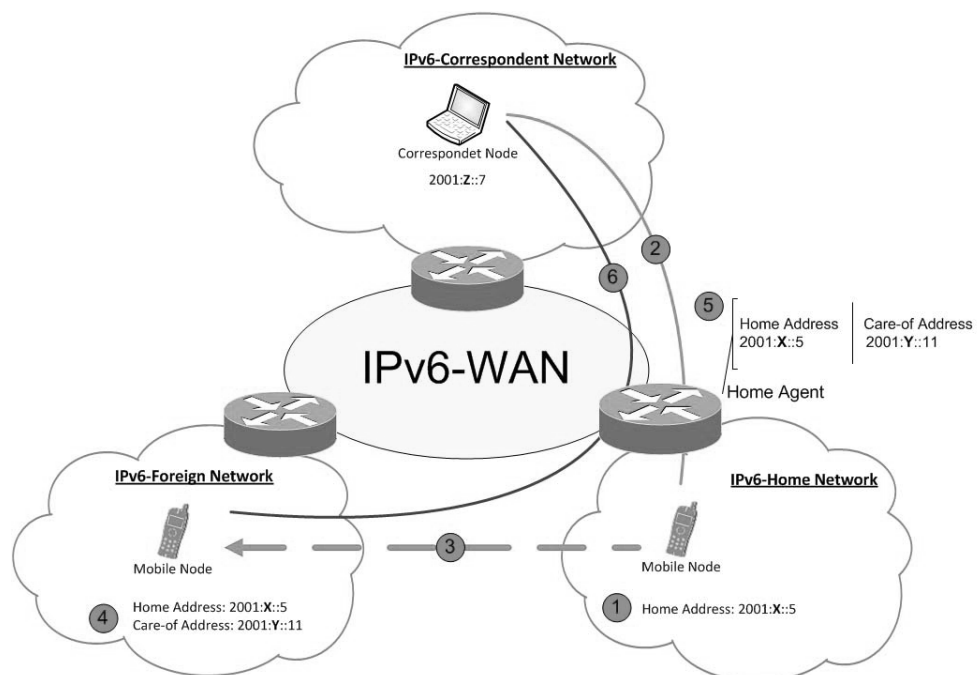

Figure 1. Movement in MIPv6 networks[7]

3.3. 6to4 Technique

6 to 4 technique [8] is an Internet transition mechanism for migrating from IPv4 to IPv6, a system that allows IPv6 packets to be transmitted over an IPv4 network (generally the IPv4 Internet) without the need to configure explicit tunnels. Special relay servers are also in place that allow 6to4 networks to communicate with native IPv6 networks.

6to4 is especially relevant during the initial phases of deployment to full, native IPv6 connectivity, since IPv6 is not required on nodes between the host and the destination. However, it is intended only as a transition

mechanism and is not meant to be used permanently.

6to4 may be used by an individual host, or by a local IPv6 network. When used by a host, it must have a

global IPv4 address connected, and the host is responsible for encapsulation of outgoing IPv6 packets and decapsulation of incoming 6to4 packets. If the host is configured to forward packets for other clients, often a local network, it is then a router.

3.3.1. 6to4 addressing

As defined by [9] , and for any 32-bit global IPv4 address that is assigned to a host, a 48-bit 6to4 IPv6 prefix can be constructed for use

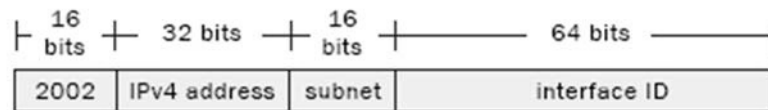by that host by appending the IPv4 address to `2002::/16` fig (2).

Figure 2: 6to4 scheme general address

For example, the global IPv4 address `193.88.99.44` has the corresponding 6to4 prefix `2002:c158:632e: :/48.or` it can be used without changing to hexadecimal like `2002: 193.88.99.44: :/48` and full address in both cases when using subnet = 1 and interface Id =1 is like figure 3.
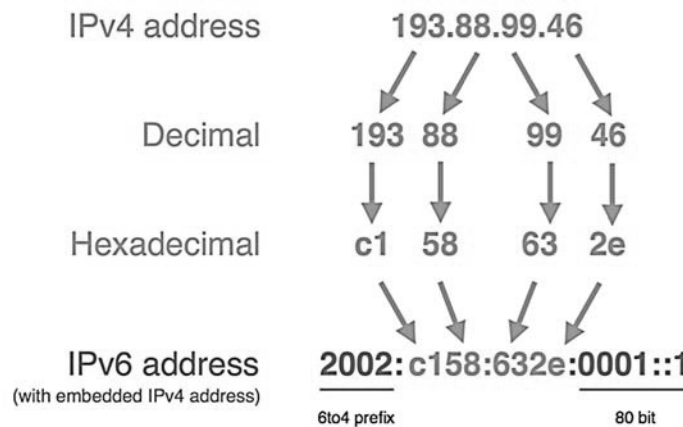

Figure 3: 6to4 address example [9]

4. Practical Study Scenarios
4.1. Practical Working Scenarios:
We used OPNET 14.5 simulation to implement these scenarios:

4.1.1. Scenario 1: MN (MIPv6) moves with IPv4 networks using 6 to 4
There are two 6to4 sites in the network, Site A and Site C. They are connected to the IPv4 backbone as shown in fig 4. 6to4 tunnels are configured on both Routers A and C enabling them to communicate with each other. The 6to4 addresses in Site A are created from the IPv4 address 192.0.4.1 which is the address of Router A interface that connects to the IPv4 backbone.

To communicate with non-6to4 IPv6 destinations, these sites use an ISP Relay (Site B). Both Routers A and C have a default route to Router B. So packets going from a 6to4 site (e.g. Site A) to a native IPv6 site (e.g. Site D) will be first tunnelled to Router B using 6to4 tunnelling and then forwarded to the eventual destination.

All routers in the native IPv6 network have a static route to the destination (2002::/16) with the next hop set to Router B. So if any of these routers receives a packet destined for a node in Sites A or C, it will be forwarded to Router B, who will be able to tunnel the packet correctly.

MN moves between Router D and Router F which located in native IPv6 using MIPv6 protocol.
All workstation nodes and mobile node MN in the network are running some application or the other.
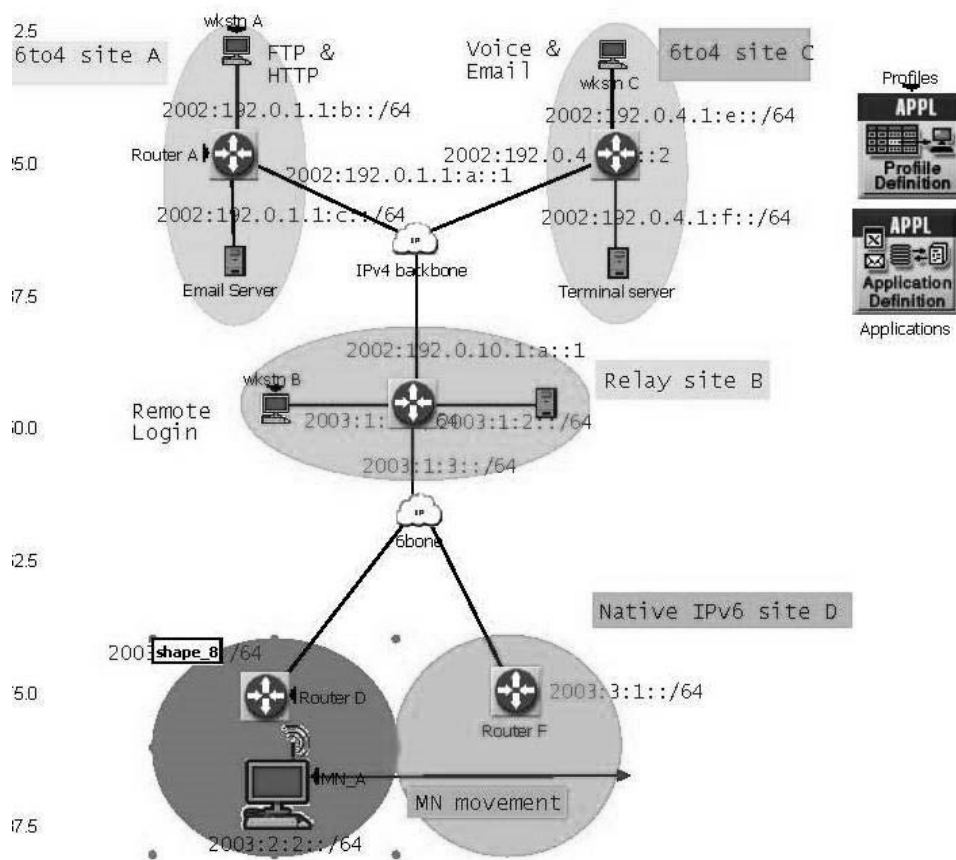

Figure 4. 6to4 address example

4.1.2. Scenario 2: MN (MIPv6) moves with pure IPv6 networks

In this case we use in all sites A, B, C, and D IPv6 networks and MN moves between Router D (HA router) to Router F using MIPv6 protocols. Like first scenario all workstation nodes and mobile node MN in the network are running some application or the other.

4.2. Practical working Hypothesis:

- **IP addresses**: All IP explained figure 4.
- **Applications**: Email (TCP connections), FTP (heavy FTP), Voice (Telephone voice), Remote login .
- **IP cloud characters (IPv4, 6 bone): we** using last load on the internet using [10] fig (5) between 24-11-2016 until 24-12-2015.
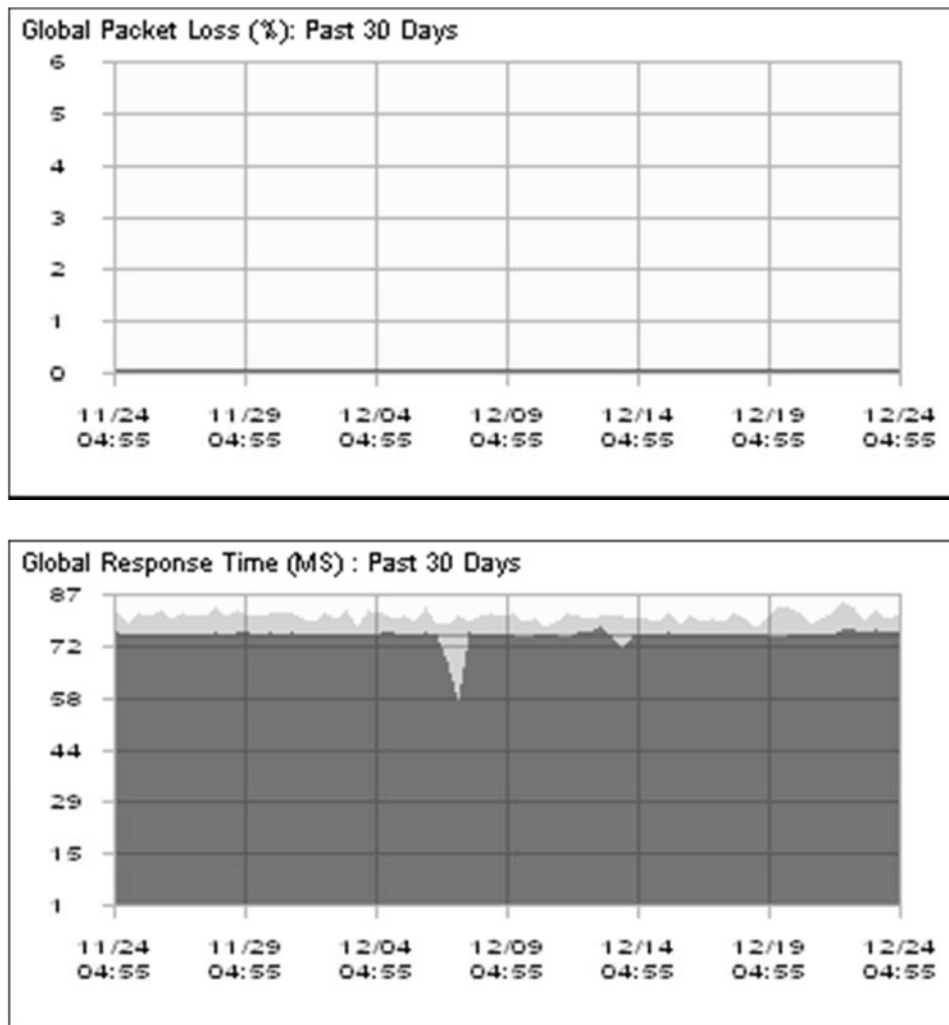

Figure 5. Internet traffic reports [10]

4.3.   Measured Parameters:

Vary parameters for different nodes has measured to get many resulted in two scenarios.

4.3.1.MN:

IPv6 Traffic Dropped:

From Figure 6 we can a traffic dropped which is the number of IPv6 datagrams dropped per second by MN node across all IP interfaces is the same but in IPv6 networks needs more traffic controls especially for neighbour discovery process.
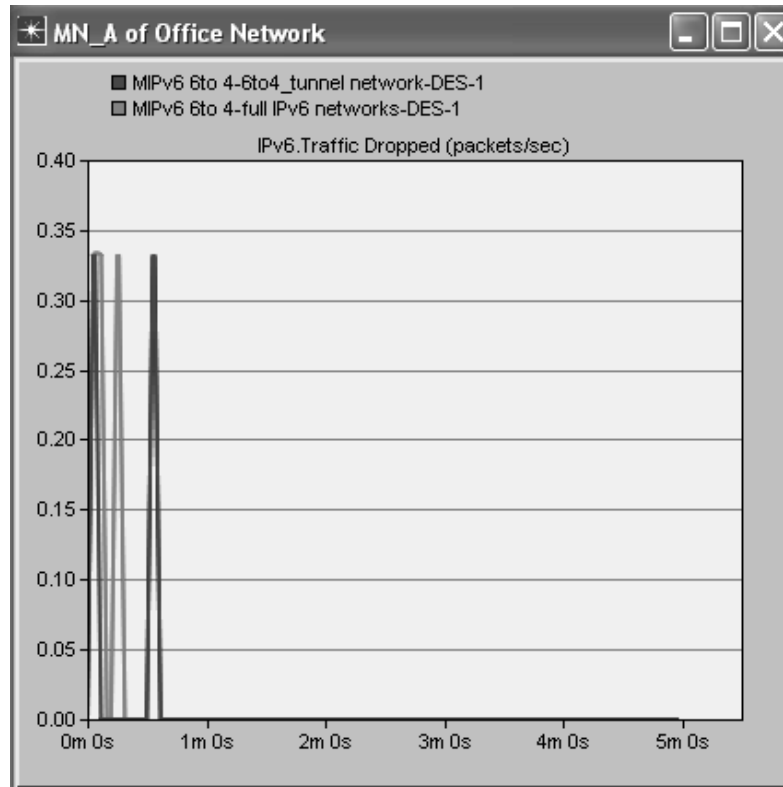

Figure 6. Traffic Dropped

IPv6 Traffic Sent /Received:

From fig 7 below we can see that MN in pure IPv6 Networks receive and sent data bigger than 6to 4 network about 150 %. This is because of avoiding packets tunnelling in IPv4 networks.
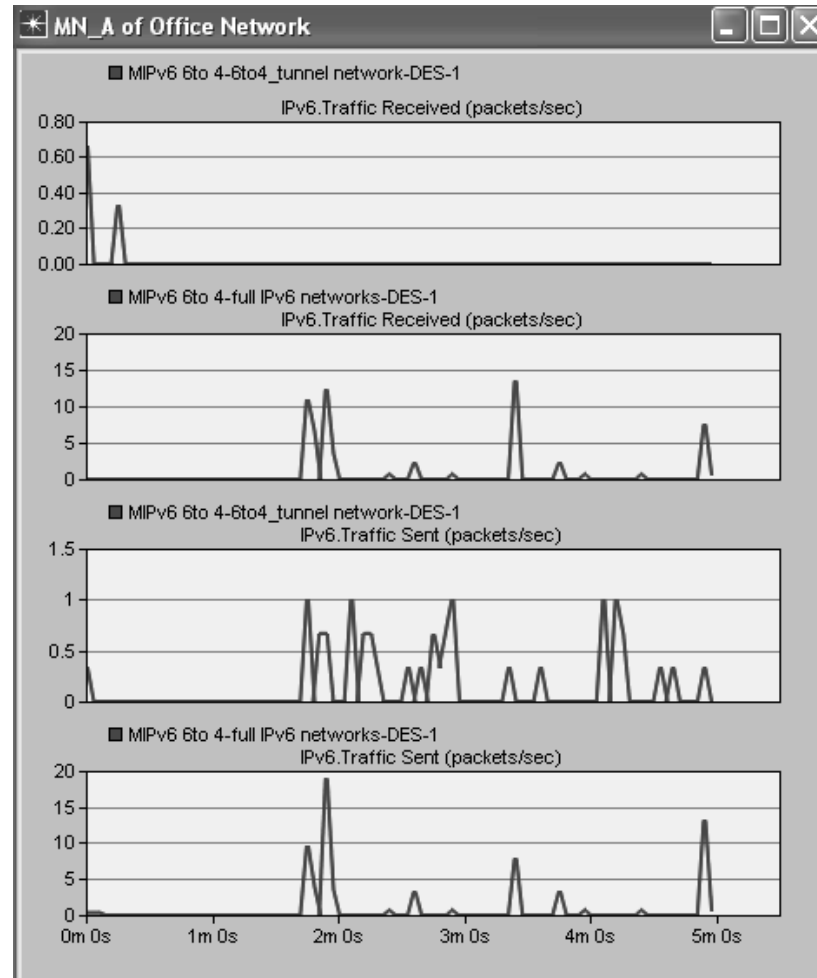
Figure 7: IPv6 Traffic Sent /Received in MN

4.3.2.Internet clouds (IPv4 and IPv6 clouds):
Fig 8 below shows that traffic sent and receive in IPv6 cloud (6 bone) and IPv4 clouds. Figure 8 shows that IPv6 datagram that sent and received in pure IPv6 scenario is bigger than ones in 6 to 4 scenario about 20 times. We can explain that because of pure IPv6 network does not need to change IP datagram's addresses between IPv4 and IPv6. Otherwise in IPv4 clouds there is no major changes between two scenarios because all converting operations between IPv6 to IPv4 process before in IPv6 cloud.
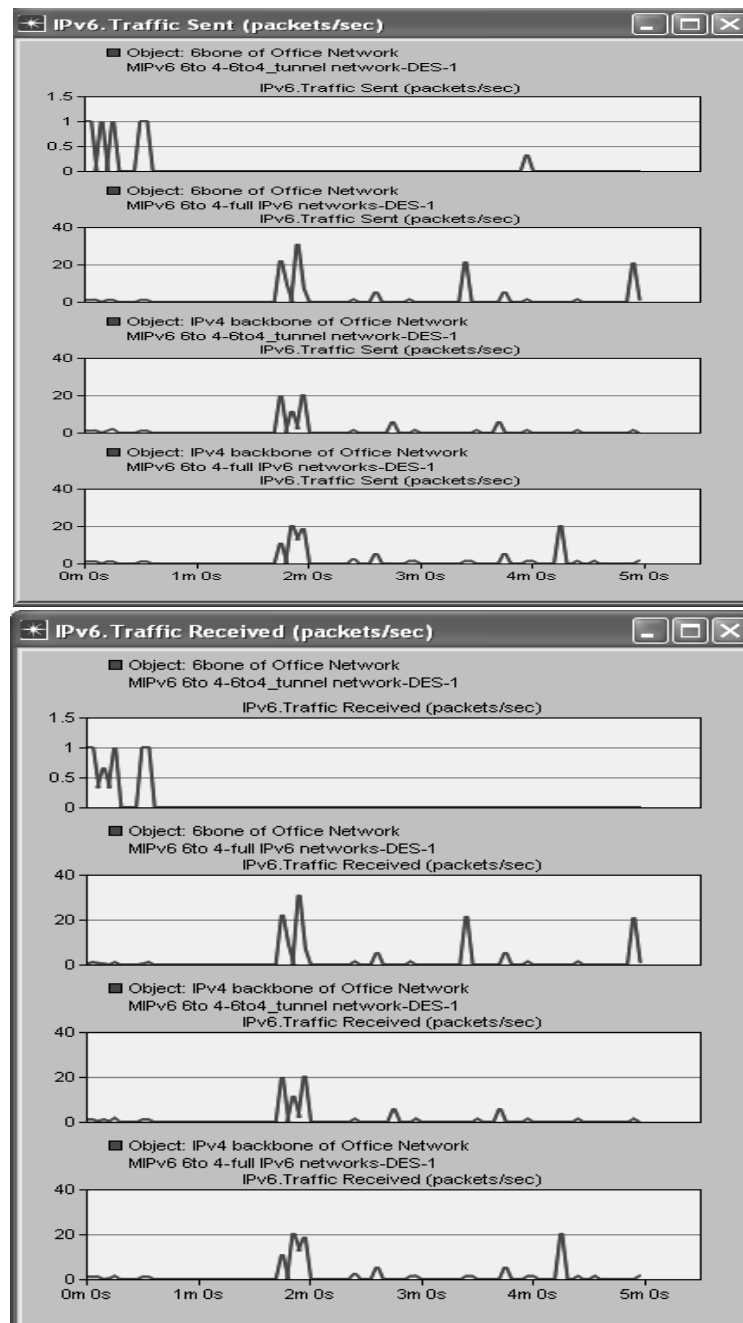
Figure 8: IPv6 Traffic Sent / Receive in IPv4 and IPv6 clouds

4.3.3.Wireless LAN:
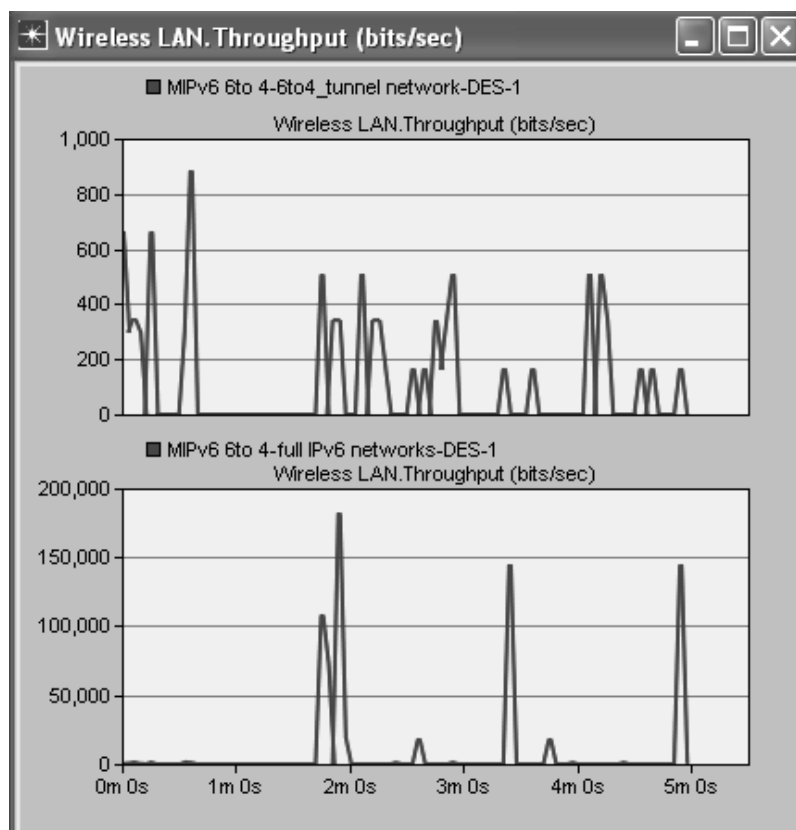**Throughput**:
According to Blum [11]: Throughput is one of the most common metrics used in the study of network Fig 9 shows that throughput in pure IPv6 networks is bigger than 6 to 4 networks with about 150% and there is no load consistently like 6 to 4 IPv6 scenario.

performance evaluation. It helps to understand the amount of data travel across a network connection or between two network hosts.

Figure 9: Throughput in WLAN

5. Results and conclusion

In this paper we have evaluated traffic sent/received and data dropped for MN inside two different kids on networks pure IPv6 and 6 to 4 IP networks. Other important parameters related to IPv6 has been noticed is throughput inside WLAN and Finally traffic load inside IPv6 internet cloud and IPv4 internet cloud which is connected to IPv6 internet clouds (6bone). The results show that working in pure IPv6 network with heavy application is better than working with IPv4/IPv6 networks that uses 6 to 4 mechanism to connect between different kinds of network with about 150%.

REFERENCES

[1] R. Hinden,   S. Deering, "IP Version 6 Addressing Architecture", IETF, RFC 4291 , February 2006, available at https://tools.ietf.org/html/rfc4291, last accessed date :25/12/2015.

[2] J. Davies ,"Understanding IPv6",Microsoft Press; 3 edition, June, 2012.

[3] Abdulkader Omar Alwer ," The Migration from Protocol IPv4 to IPv6 Mechanism , implementation & Cost" , Alba'ath University Journal, Syria,2007 available online :

http://178.253.94.33/magazine/folders/resear ches/detail_id.php?newsid=815 last accessed date :25/12/2015.

[4] A.Ahmed , A. Mustafa, G. Ibrahim, "Performance Evaluation of IPv4 Vs Ipv6 and Tunnelling Techniques Using Optimized Network Engineering Tools (OPNET)" , IOSR Journal of Computer Engineering (IOSR-JCE); Volume 17, Issue 1, Ver. IV (Jan – Feb. 2015), PP 72-75.2007 available online :http://www.iosrjournals.org/iosr-

jce/papers/Vol17-issue1/Version-4/M017147275.pdf.

[5] Oliveira L., Amaral A., de Sousa, A.F., "Mobility in IPv4–IPv6 Transition Scenarios", 4th Conferência de Telecomunicações (ConfTELE), Aveiro, Portugal, June 2003. available online: http://www.av.it.pt/asou/papers/oliveiraConf Tele03.pdf.

[6] C. Perkins,D. Johnson, J. Arkko, "Mobility Support in IPv6" ,IETF, RFC 6275 , July 2011, available at https://tools.ietf.org/html/rfc6275 , last accessed date :25/12/2015.

[7] R .Kodli, C.Perkins ," Mobile Internetworking with IPv6" ,Wiley ,New Jersey, USA, July 2007, ISBN: 978-0-471-68165-6.

[8] E. Nordmark , R. Gilligan , " Basic Transition Mechanisms for IPv6 Hosts and Routers", IETF, RFC 4213 , October 2005, available at https://tools.ietf.org/html/rfc4213,last accessed date :25/12/2015.

[9] B. Carpenter , K. Moore ," Connection of IPv6 Domains via IPv4 Clouds" , IETF, RFC 3056 , February 2001 , available at https://tools.ietf.org/html/rfc3056 , last accessed date :25/12/2015.

[10] http://www.internettrafficreport.com/30day.h tm.

[11] R.Blum,"Network performance open source toolkit: Using Netperf, tcptrace, NIST Net, and SSFNet"Wiley, 2003.

SUBMISSION INSTRUCTIONS

The scope of International Journal of Electronics, Mechanical and Mechatronics Engineering (IJEMME) covers the novel scientific papers about Electronics, Image Processing, Information Theory, Electrical Systems, Power Electronics, Control Theory, Embedded Systems, Robotics, Motion Control, Stochastic Modeling, System Design, Multidisciplinary Engineering, Computer Engineering, Optical Engineering, Design Optimization, Material Science, Metamaterials, Heat and Mass Transfer, Kinematics, Dynamics, Thermo-Dynamics, Energy and Applications, Renewable Energy, Environmental Impacts, Structural Analysis, Fluid Dynamics and related topics of the above subjects.

IJEMME is an international periodical published triple a year (February, July and October). Manuscripts reporting on original theoretical and/or experimental work and tutorial expositions of permanent reference value are welcome. IJEMME Editorial Board is authorized to accept/reject the manuscripts based on the evaluation of international experts. The papers should be written in English.
The manuscript should be sent in electronic submission via **zaferutlu@aydin.edu.tr**

SUBMISSION INSTRUCTIONS OF MANUSCRIPTS.

Page Design: Text body area is (195mm x 275mm). 30 mm margin from top, 20 mm from down and 25 mm margin should be left on right/left sides.

Title: should be in 16 pt. bold, capital letters with Times New Roman font in Microsoft Word format. Authors' names, affiliations, e-mail addresses should follow the title after double line spacing with authors' names and surnames in lower case except first letters in 14 pt, the rest is 10 pt. italic.

Abstract: should not exceed 200 words with the word "Abstract" in 10 pt. italic, bold, abstract text in 9 pt. italic, all in Times New Roman font in Microsoft Word format.

Keywords: not exceeding 5 should be in bold.

Document Character: Subtitles should be in 10 pt. bold, capital letters and text body 10 pt. both with Times New Roman font in Microsoft Word format. The manuscripts should be written on a single column, be double spaced with single line spacing between paragraphs. The subtitle of the first section should start after a single space following the keywords, the other subtitles also with a single line space following the text, there should also be single line spacing between the previous text and the subtitle.

CONCLUSION section should have a title written in 1o pt. bold, capital letters and the text in 10 pt. all in Times New Roman font in Microsoft Word format.
REFERENCE numbers should be given in brackets as illustrated below:
Referencing books:

[1] Özsu M., T, Valduriez, P., Principles of Distributed Database Systems, Prentice Hall, New Jersey, 128-136,1991.

Referencing papers:

[2] G. Altay, O. N., Ucan, "Heuristic Construction of High-Rate Linear Block Codes," International Journal of Electronics and Communications (AEU), vol. 60, pp.663-666, 2006.

Page number is to be placed at the top left corner of each page with pencil.
Length of the Manuscript should not exceed 20 pages excluding Figures and Tables.

INSTRUCTIONS ABOUT THE ACCEPTED MANUSCRIPTS:

Page Design: Text body area is (195mm x 275mm). 30 mm margin from top, 20 mm from down and 25 mm margins should be left on right/left sides.

Title: should be in 16 pt. bold, capital letters with Times New Roman font in Microsoft Word format. Authors' names, affiliations, e-mail addresses should follow the title after double line spacing with authors' names in lower case and surnames in capital letter in 14 pt. the rest in 10 pt. in the same format.

Abstract: should not exceed 200 words with the word "Abstract" in 12 pt. italic, bold, abstract text in 9 pt. italic, all in Times New Roman font in Microsoft Word format.

Keywords: not exceeding 5 should be in 9 pt. bold.

Document Character: Subtitles should be in 10 pt. bold, capital letters and text body 10 pt. both with Times New Roman font in Microsoft Word format. **The manuscripts should be written on two columns, be single spaced with single line spacing between paragraphs.** The subtitle of the first section should start after a single space following the keywords, the other subtitles also with a single line space following the text, there should also be single line spacing between the previous text and the subtitle.

SECTIONS: Formulas should be numbered sequentially. Referring to formulas should be as Eqn (.). Figures and Tables should be placed into the text body and captions for both should be 10 pt. Table numbers and captions should be placed before the Table. If necessary, both columns may be used for large Figures and Tables.

CONCLUSION section should have a title written in 12 pt. bold, capital letters and the text in 10 pt. all in Times New Roman font in Microsoft Word format. Conclusion should not be a version of the Abstract.
REFERENCE numbers should be given in brackets as illustrated below:

Referencing books:
[1] Özsu M., T, Valduriez, P., Principles of Distributed Database Systems, Prentice Hall, New Jersey, 128-136,1991.

Referencing papers:

[2]G. Altay, O. N., Ucan, "Heuristic Construction of High-Rate Linear Block Codes," International Journal of Electronics and Communications (AEU), vol. 60, pp.663-666, 2006.

SHORT BIOGRAPHY of the authors should follow references after a single line space, names in 9 pt. surnames in 9 pt. and the text in 9 pt. The text should not exceed 100 words.

CORRESPONDENCE ADDRESS:

Editor
Prof. Dr. Zafer UTLU
Engineering Faculty
Mechanical Engineering Department
Inonu Caddesi, No.38, Florya, Istanbul, TURKEY
E-mail: zaferutlu@aydin.edu.tr
Web : www.aydin.edu.tr/eng/ijemme

Prepared by
Instructor: Şenay KOCAKOYUN
Anadolu BIL Vocational High School
Computer Programming Department
Inonu Caddesi, No.38 Florya, Istanbul, TURKEY
E-mail: senaykocakoyun@aydin.edu.tr

Published by
Istanbul Aydın University